

Accumulation of Herpes Simplex Virus Type 1 Early and Leaky-Late Proteins Correlates with Apoptosis Prevention in Infected Human HEp-2 Cells

MARTINE AUBERT,¹ STEPHEN A. RICE,² AND JOHN A. BLAHO^{1*}

Department of Microbiology, Mount Sinai School of Medicine, New York, New York 10029,¹ and Department of Microbiology, University of Minnesota Medical School, Minneapolis, Minnesota 55455²

Received 29 August 2000/Accepted 23 October 2000

We previously reported that a recombinant ICP27-null virus stimulated, but did not prevent, apoptosis in human HEp-2 cells during infection (M. Aubert and J. A. Blaho, *J. Virol.* 73:2803–2813, 1999). In the present study, we used a panel of 15 recombinant ICP27 mutant viruses to determine which features of herpes simplex virus type 1 (HSV-1) replication are required for the apoptosis-inhibitory activity. Each virus was defined experimentally as either apoptotic, partially apoptotic, or nonapoptotic based on infected HEp-2 cell morphologies, percentages of infected cells with condensed chromatin, and patterns of specific cellular death factor processing. Viruses *d27-1*, *d1-5*, *d1-2*, M11, M15, M16, *n504R*, *n406R*, *n263R*, and *n59R* are apoptotic or partially apoptotic in HEp-2 cells and severely defective for growth in Vero cells. Viruses *d2-3*, *d3-4*, *d4-5*, *d5-6*, and *d6-7* are nonapoptotic, demonstrating that ICP27 contains a large amino-terminal region, including its RGG box RNA binding domain, which is not essential for apoptosis prevention. Accumulations of viral TK, VP16, and gD but not gC, ICP22, or ICP4 proteins correlated with prevention of apoptosis during the replication of these viruses. Of the nonapoptotic viruses, *d4-5* did not produce gC, indicating that accumulation of true late gene products is not necessary for the prevention process. Analyses of viral DNA synthesis in HEp-2 cells indicated that apoptosis prevention by HSV-1 requires that the infection proceeds to the stage in which viral DNA replication takes place. Infections performed in the presence of the drug phosphonoacetic acid confirmed that the process of viral DNA synthesis and the accumulation of true late (γ_2) proteins are not required for apoptosis prevention. Based on our results, we conclude that the accumulation of HSV-1 early (β) and leaky-late (γ_1) proteins correlates with the prevention of apoptosis in infected HEp-2 cells.

The expression of herpes simplex virus type 1 (HSV-1) genes occurs through a highly regulated cascade (23) beginning with the production of the α or immediate-early (IE) proteins. The α regulatory proteins, infected cell proteins 0, 4, 22, and 27, cooperatively act to regulate the expression of all classes of viral genes (reviewed in reference 52). The β or early (E) gene products, such as the viral thymidine kinase (TK), are synthesized next and are the proteins principally involved in viral DNA synthesis (reviewed in reference 7). The last set of viral proteins produced are the γ or late (L) proteins and are mainly associated with virion structure and assembly, such as the VP16, gD, and gC proteins (4, 15, 47). The γ gene class is further subdivided into the γ_1 and γ_2 groups, where γ_2 expression is absolutely dependent on viral DNA synthesis. The completion of the HSV-1 replication cycle leads ultimately to the destruction of the cells in culture, and this process is generally believed to occur through a necrotic route. Consequently, productive HSV-1 replication induces major biochemical and morphological alterations (3, 18, 21, 52). However, features observed with wild type HSV-infected cells are different from those associated with cells dying from apoptosis. Apoptotic cells are characterized by cellular changes that include cell shrinkage, membrane blebbing, nuclear condensation, and

fragmentation of chromosomal DNA into nucleosomal oligomers (reviewed in reference 28).

Previously, we reported that human epithelial cells present characteristic morphological and biochemical hallmarks of apoptotic cells when infected with an HSV-1 ICP27-null mutant virus (1, 2). These apoptotic features include membrane blebbing and the formation of apoptotic bodies. A time-lapse movie showing infected-cell apoptosis is available at our public domain website (<http://www.mssm.edu/micro/blaho/webdata/maetaldns.shtml>). In addition, we detected chromatin condensation, nuclear fragmentation, and nucleosomal laddering in ICP27-null-virus-infected cells. Finally, we determined that these defining features of apoptosis proceed through a pathway in which caspase-3 is activated and the death substrates DNA fragmentation factor (DFF) and poly(ADP-ribose) polymerase (PARP) are processed. These features are not observed with wild type-infected cells unless total protein synthesis is inhibited by the addition of cycloheximide during infection (1, 2, 30). From these results, we concluded that both wild-type and ICP27-null viruses induce apoptosis in human cells, but the ICP27-null virus is not able to prevent the apoptotic process from killing the cells.

ICP27 is a multifunctional phosphoprotein which is necessary for completion of the viral lytic cycle (32, 48, 53, 67, 69). During infection, ICP27 stimulates both E (β) gene and L (γ) gene expression (19, 32, 48, 53, 55, 56, 65) and down-regulates IE (α) and E gene expression at late times (32, 48, 53). In addition, ICP27 significantly enhances the efficiency of viral

* Corresponding author. Mailing address: Department of Microbiology, Mount Sinai School of Medicine, One Gustave L. Levy Place, New York, NY 10029. Phone: (212) 241-7318. Fax: (212) 534-1684. E-mail: john.blaho@mssm.edu.

TABLE 1. Features of the recombinant viruses used in this study

Virus	Source or reference	Mutation		Amino acid(s) affected	Viral DNA replication	Nuclear localization
		Type	Domain(s)			
KOS1.1	24	None	None	None	Wild type	N, Nu, shuttles ^b
<i>d27-1</i>	48	Deletion	All	1–512	Defective (49)	ND
<i>d1-5</i>	38	Deletion	Amino	13–153	ND ^a	ND
<i>d1-2</i>	50	Deletion	Amino	12–63	Defective (50)	N, shuttling reduced (37)
<i>d2-3</i>	This study	Deletion	Amino	64–109	ND	ND (38)
<i>d3-4</i>	36	Deletion	Amino	109–138	ND	N > C (38)
<i>d4-5</i>	36	Deletion	Amino	139–153	ND	N, not Nu (38)
<i>d5-6</i>	38	Deletion	Amino	154–173	ND	ND
<i>d6-7</i>	This study	Deletion	Amino	174–200	ND	ND
M11	49	Point, RD to LE	Carboxy	340, 341	Wild type (49)	N, shuttling reduced (37, 38)
M15	49	Point, PG to LE	Carboxy	465, 466	Wild type (48)	N, no shuttling (37)
M16	49	Point, C to L	Carboxy	488	Wild type (49)	N, shuttling reduced (37)
<i>n504R</i>	48	Nonsense	Carboxy	505–512	Wild type (48, 49)	N diffuse (48, 50), shuttle (37)
<i>n406R</i>	48	Nonsense	Carboxy	407–512	Defective (49)	N punctate, not Nu (48, 51)
<i>n263R</i>	48	Nonsense	Carboxy	264–512	Defective (49)	N, preferentially Nu (48, 51)
<i>n59R</i>	48	Nonsense	Carboxy	60–512	Defective (49)	Protein not detected (45, 51)

^a ND, not determined.

^b N, nuclear; Nu, nucleolar.

DNA replication (32, 48), most likely by increasing the expression of viral DNA replication factors (33, 65). The ability of ICP27 to stimulate DNA replication is separable, by mutation, from its stimulatory effect on L genes (48, 49, 53). The regulatory effects of ICP27 can also be demonstrated in uninfected cells, as ICP27 can enhance or repress reporter genes in transient expression assays (19, 51, 59). Although the mechanism of action of ICP27 is as yet unknown, there is a great deal of evidence to suggest that it regulates gene expression posttranscriptionally through the modulation of mRNA processing and export. ICP27's known posttranscriptional activities include (i) modulation of pre-mRNA polyadenylation efficiency (33, 34, 58), (ii) binding and stabilization of the labile 3' ends of mRNA (8), (iii) redistribution of pre-mRNA splicing factors such as snRNPs (41, 57), (iv) inhibition of cellular and viral pre-mRNA splicing (20), and (v) nuclear retention of intron-containing viral transcripts (43, 56). Consistent with these activities is ICP27's ability to bind RNA (8, 25, 38) and to shuttle between the nucleus and cytoplasm (37, 42, 56, 60).

The timing of these well-documented regulatory functions of ICP27 is consistent with our observation that the apoptosis prevention function present during wild-type HSV-1 infection is detected after 3 h postinfection (p.i.) (2). The goal of this study was to define more precisely the features of viral replication which are involved in apoptosis prevention during HSV-1 infection of human epithelial cells. Using a series of recombinant HSV-1 viruses which possess deletion, nonsense, or point mutations in the gene encoding ICP27, we infected cultured HEP-2 cells and documented the extent of apoptosis for each virus. Analyses of cell morphology, cellular death factor processing, viral protein accumulation, viral DNA synthesis, and productive viral replication were performed. Our findings indicate that the accumulation of early (β) and leaky-late (γ_1), but not true late (γ_2), viral gene products correlates with apoptosis prevention during HSV-1 infection. Based on these results, we suggest that ICP27 regulates the synthesis of the viral proteins which participate in the blocking of apoptosis during HSV-1 infection.

MATERIALS AND METHODS

Cell lines and viruses. All cells were maintained in Dulbecco's modified Eagle's medium containing 5% fetal bovine serum. HEP-2 and Vero cells were obtained from the American Type Culture Collection (Rockville, Md.). V27 is a derivative Vero cell line which carries a stably integrated copy of the ICP27 gene (48). HEP-2 cell monolayers were infected at a multiplicity of infection (MOI) of 10 PFU/cell, and the infections were maintained at 37°C in Dulbecco's modified Eagle's medium with 5% newborn calf serum for 24 h. For viral growth determination, Vero cells (2.2×10^6) were infected at an MOI of 10 PFU per cell. The same inocula were used to infect parallel cultures of 2.5×10^6 V27 cells. The cultures were harvested at 24 h p.i., and virus yield was determined by plaque assay on V27 cells. KOS1.1 (24) is the wild-type parental virus, and the features of all the recombinant viruses used in this study are described in detail in Table 1 and Fig. 1. The mutants *d27-1*, *n59R*, *n263R*, *n406R*, *n504R*, *d1-2*, *d3-4*, *d4-5*, *d5-6*, *d1-5*, M11, M15, and M16 have been described (36, 38, 49, 50). Construction of the *d2-3* and *d6-7* viruses was analogous to that of the *d3-4* and *d4-5* viruses (36). Two independent plaque isolates (a and b) of *d1-2* and *d4-5* were analyzed.

Infected cell extract preparations, denaturing gel electrophoresis, and transblotting. Whole extracts of infected cells were obtained as described previously (1). Protein concentrations were measured using a modified Bradford assay (Bio-Rad) as recommended by the vendor. Equal amounts of infected cell proteins (50 μ g) were separated in denaturing 15% *N,N'*-diallyltartardiamide (DATD)-acrylamide gels (1) and electrically transferred to nitrocellulose membranes in a tank apparatus (Bio-Rad) prior to immunoblotting with various primary antibodies. Unless otherwise noted in the text, all biochemical reagents were obtained from Sigma. Nitrocellulose was obtained directly from Schleicher & Schuell. Protein molecular weight markers (not shown in figures) and all tissue culture reagents were purchased from Life Technologies.

Immunological reagents. The following primary antibodies were used to detect viral proteins: (i) RGST22, rabbit antibody specific for full-length ICP22 (6); (ii) rabbit anti-TK polyclonal antibody (gift of Bernard Roizman); (iii) VP16(1-21), mouse anti-VP16 monoclonal antibody (Santa Cruz Biotechnology, Inc.); (iv) H1119, mouse anti-ICP27 monoclonal antibody; (v) H1114, mouse anti-ICP4 monoclonal antibody; (vi) H1103, mouse anti-glycoprotein D (gD) monoclonal antibody; and (vii) H1104, mouse anti-glycoprotein C (gC) monoclonal antibody (Goodwin Institute for Cancer Research, Plantation, Fla.). Cellular proteins were detected by using mouse anti-caspase-3 monoclonal antibody (Transduction Laboratories, Inc.), mouse anti-PARP monoclonal antibody (Pharmingen), and goat anti-DFF polyclonal antibody (Santa Cruz Biotechnology, Inc.). Mouse anti- α tubulin monoclonal antibody (Sigma) was used to confirm equal loading of the cell extracts. Secondary (goat) anti-rabbit, anti-mouse, and (rabbit) anti-goat antibodies conjugated with alkaline phosphatase were purchased from Southern Biotechnologies Associates, Inc. (Birmingham, Ala.). Secondary (goat) anti-mouse antibody conjugated with horseradish peroxidase was obtained from Am-

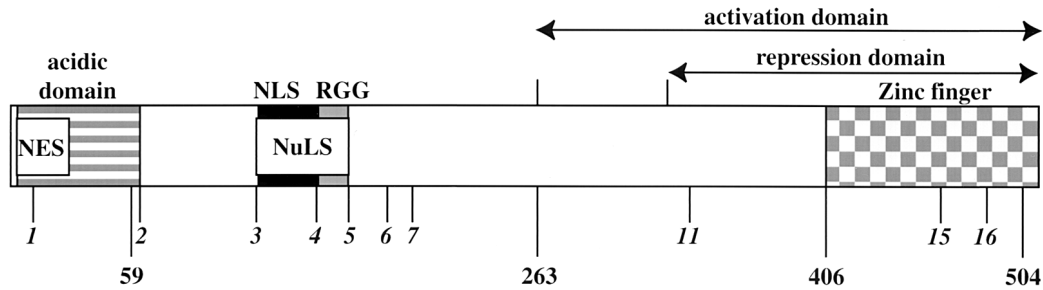


FIG. 1. Schematic of the ICP27 protein showing locations of defined functional regions. These include NES, a putative nuclear export signal (open box); the acidic domain, involved in gene expression and DNA synthesis (striped box); NLS, nuclear localization signal (black box); NuLS, nucleolar localization signal (white box); RGG sequence, RNA binding motif (gray box); and activation and repression domains (arrows), which include a cysteine-histidine zinc-finger-like domain (checkered box). Italicized numbers define mutated sites (M11, M15, and M16) and the boundaries of in-frame deletions. Bold numbers correspond to relevant amino acid positions.

erham and used for the VP16, gC, and α tubulin immunoblot analyses (chemiluminescence) presented in Fig. 4 and for gD in Fig. 7.

DNA replication assay. Approximately 10^6 Hep-2 cells were either mock infected or infected with wild-type or mutant HSV-1 at an MOI of 10 PFU/cell. After a 1-h adsorption, the cells were overlaid with 199 medium containing 2% newborn calf serum. At 2 and 20 h p.i., total infected cell DNA was isolated by the following procedure. The medium was replaced by 3 ml of lysis buffer (10 mM Tris-HCl [pH 8.0], 10 mM Na₂EDTA, 2% sodium dodecyl sulfate, 100 μ g of proteinase K/ml), and the flasks were incubated at 37°C for either 22 or 4 h. After the addition of 0.33 ml of 3 M sodium acetate, each lysate was extracted first with an equal volume of phenol-chloroform-isoamyl alcohol (25:24:1) and then with an equal volume of chloroform-isoamyl alcohol (24:1). After two sequential ethanol precipitations, the purified DNA was resuspended in TE buffer (10 mM Tris-HCl [pH 8.0], 1 mM Na₂EDTA) and its concentration was determined by UV absorbance at 260 nm. Equal amounts of each DNA preparation (6.7 μ g) were then digested with *Pst*I, electrophoresed on a 1% agarose gel, and blotted to a nylon membrane. The membrane was hybridized with a ³²P-labeled 813-bp plasmid-derived *Eco*NI/*Eco*RV restriction fragment corresponding to the coding region of the HSV-1 U_L44 (gC) gene. This probe detects a 4.7-kb HSV-1 genomic *Pst*I fragment. Hybridization, carried out overnight at 42°C in UltraHyb (Ambion), and washing were done according to the manufacturer's specifications. Quantitation of the radioactive bands was performed using a Molecular Dynamics phosphorimaging system.

Percentage of apoptotic cells. The percentages of apoptotic cells were determined as follows. Hep-2 cell monolayers grown on glass coverslips in 35-mm-

diameter dishes were infected at an MOI of 5 PFU/cell in the absence or presence of the caspase inhibitory peptide Z-Val-Ala-Asp-fluoromethyl ketone (z-VAD-fmk; Calbiochem, San Diego, Calif.) at a final concentration of 100 μ M at 37°C. At 15 h p.i., the cells were fixed with 2% formaldehyde in phosphate-buffered saline for 20 min, permeabilized with 100% acetone at -20°C for 4 min (44), and incubated with the DNA dye Hoechst 33258 (Sigma) at a final concentration of 5 μ g/ml in phosphate-buffered saline for 10 min. The number of apoptotic cells with condensed chromatin DNA and fragmented nuclei (1), as well as the total number of cells in representative fields, were counted by using an Olympus model IX70 fluorescence microscope. The percentage of apoptotic cells was calculated as follows: (number of apoptotic cells/total number of cells) \times 100. The data of Fig. 3 represent the mean of two independent experiments in which a minimum of 260 and a maximum of 325 cells were counted for each virus.

Quantitative measurements of processed proteins. The amounts of representative cellular and viral polypeptides were determined and used to define the percentage of PARP processing detected during infection as follows. Relative amounts of cellular (see Fig. 4) and viral (see Fig. 5) proteins and values of percent PARP processing (Table 2) were calculated using the public domain NIH Image program (developed at the National Institutes of Health and available on the Internet at <http://rsb.info.nih.gov/nih-image>). Immunoblots were digitized using an AGFA Arcus II scanner linked to a Macintosh G3 Power PC workstation. Raw digital images (2 in. horizontal) were saved as 8-bit gray-scale tagged image files (TIF) at a resolution of 300 dots per inch, using Adobe Photoshop version 5.0. Mean pixel measurements were calculated twice by using

TABLE 2. Comparison of apoptosis in Hep-2 cells and growth properties in Vero cell lines

Virus	% Apoptotic cells	% PARP processing	Hep-2 cell phenotype ^c	Vero cell titer (PFU/ml)	V27 cell titer (PFU/ml)	Plaquing ratio (Vero/V27)	Functional region(s) affected
KOS1.1	8	21	NA	4.8×10^8	3.0×10^8	1.6	None
d27-1	89	96	A	$<2.0 \times 10^3$	4.0×10^8	$<5.0 \times 10^{-6}$	All
d1-5	78	93	A	$<2.0 \times 10^3$	4.0×10^8	$<5.0 \times 10^{-6}$	NES, acidic domain, NLS, NuLS, RGG box
d1-2	58	84	A	$<2.0 \times 10^4$	2.8×10^8	$<7.1 \times 10^{-5}$	NES, acidic domain
d2-3	14	30	NA	4.6×10^{8a}	8.0×10^8	5.8×10^{-1}	^{*d}
d3-4	18	54	NA	7.8×10^{7b}	4.4×10^8	1.8×10^{-1}	NLS, NuLS
d4-5	17	28	NA	9.0×10^{5b}	1.9×10^8	4.7×10^{-3}	NuLS, RGG box
d5-6	12	46	NA	3.0×10^8	8.0×10^8	3.8×10^{-1}	*
d6-7	9	31	NA	2.2×10^8	6.0×10^8	3.7×10^{-1}	*
M11	36	71	PA	4.2×10^3	1.4×10^8	3.0×10^{-5}	Activation/repression domain
M15	56	86	A	$<2.0 \times 10^2$	1.8×10^8	$<1.1 \times 10^{-6}$	Activation/repression domain
M16	31	58	PA	4.0×10^2	1.0×10^8	4.0×10^{-6}	Activation/repression domain, putative zinc finger
n504R	42	80	PA	$<2.0 \times 10^2$	8.8×10^7	$<2.3 \times 10^{-6}$	Activation/repression domain, putative zinc finger
n406R	35	54	PA	$<2.0 \times 10^2$	1.3×10^8	$<1.5 \times 10^{-6}$	Activation/repression domain, putative zinc finger
n263R	69	91	A	$<2.0 \times 10^2$	1.0×10^8	$<2.0 \times 10^{-6}$	Activation/repression domain, putative zinc finger
n59R	78	94	A	$<2.0 \times 10^2$	1.6×10^8	$<1.3 \times 10^{-6}$	Acidic domain, NLS, NuLS, RGG box, putative zinc finger, activation/repression domain

^a Small plaques.

^b Minute plaques.

^c NA, nonapoptotic; A, apoptotic; PA, partially apoptotic.

^d *, no function defined.

NIH Image software and averaged. Analysis areas were held constant and were 0.11 by 0.03 in. for PARP and processed PARP, 0.12 by 0.04 in. for caspase-3 and TK, and 0.12 by 0.07 in. for VP16. Percent PARP processing was defined as the percent conversion of full-length PARP (molecular weight, 116,000) to processed PARP (molecular weight, 85,000) $\{[\text{processed PARP}/(\text{PARP} + \text{processed PARP})] \times 100\}$. Amounts of PARP and caspase-3 were relative to that in mock-infected cells (100%). Processed PARP was relative to that measured with *d27-1*. TK and VP16 were relative to that measured with KOS1.1. As we reported previously, the observed amounts of unprocessed and processed PARP for any given infection are not molarly equivalent due to their differences in transfer efficiency (2). Thus, either the relative amounts of each form or the ratios of the two forms are comparable between each infection. Finally, all values were normalized to the amount of α tubulin present in each lane to eliminate any potential error due to differences in sample loadings.

Microscopy and computer graphics. Infected-cell phenotypes were documented by phase-contrast light microscopy using an Olympus CK2/PM-10AK3 system with an attached 35 mm camera. Immunoblots, autoradiograms, and 35 mm slides were digitized at a resolution of 800 to 1,000 dots per inch as described above. Raw digital images (TIF format) were organized using Adobe Illustrator version 7.1, and gray-scale prints of figures were obtained by using a Codonics dye sublimation printer. Time-lapse photography was performed on a Zeiss Axioskop phase-contrast microscope linked to a PowerMac G3. Digital images were captured at 5-min intervals, converted to TIFs using Photoshop, and organized into a movie using Quicktime 4.1. Certain results may be accessed through our website (<http://www.mssm.edu/micro/blaho/webdata/maetaldns.shtml>).

RESULTS

Recombinant viruses with defined mutations in ICP27 functional regions. Previously (1), we demonstrated apoptosis during the infection of human cells with a mutant virus possessing a complete deletion of the gene encoding ICP27 (i.e., $\nu\text{BS}\Delta 27$). In this study, we set out to test whether different ICP27 mutant recombinant viruses carrying partial deletions, nonsense mutations, or point mutations in the ICP27 gene (Table 1) retain their ability to prevent apoptosis compared to the HSV-1 ICP27-null virus phenotype. Since infection with a virus containing a complete ICP27 deletion leads to apoptosis, all recombinant viruses tested in our study have the ability to induce this process. Therefore, we were interested in identifying which mutant viruses are unable to block the process as a consequence of their lesion in ICP27. Our goal is to use this series of recombinant viruses to identify the features of viral replication which participate in the prevention of apoptosis during HSV-1 infection of human epithelial cells.

Wild-type KOS1.1 is the parental strain of all of the recombinant viruses used in this study. The *d27-1* virus (48) is equivalent to the $\nu\text{BS}\Delta 27$ virus (60) used in our earlier studies since both viruses carry large deletions in the ICP27 gene and are null for ICP27 function. The viruses *d1-5*, *d1-2*, *d2-3*, *d3-4*, *d4-5*, *d5-6*, and *d6-7* (Table 1) produce truncated forms of ICP27, and their deletions map in the amino half of the protein. This portion of ICP27 (Fig. 1) contains defined functional regions (amino domains) including a nuclear export signal, NES (56), nuclear and nucleolar localization signals, NLS and NuLS, respectively (22, 36), and an arginine- and glycine-rich RGG box RNA binding motif (38, 56). The acidic amino acid region (acidic domain) at the beginning of the amino half of ICP27 contributes to its gene regulation and DNA replication functions (50). All of the remaining recombinant viruses have mutations which affect the other half (carboxy domain) of ICP27. M11, M15, and M16 contain point mutations, while *n59R*, *n263R*, *n406R*, and *n504R* are nonsense mutants which express ICP27 molecules with the carboxy terminus deleted (Table 1 and Fig. 1). The carboxy domain of ICP27 contains a

potential zinc finger metal binding motif (66) and is required during viral infection for efficient L gene expression and viral DNA synthesis (35, 48, 49). In addition, this part of the molecule possesses the "activation" and "repression" domains, originally defined by Sandri-Goldin and colleagues (19), which are critical to ICP27's ability to stimulate and repress the expression of cotransfected reporter genes in transient expression assays (9, 19, 35, 49, 51, 59). Recently, the carboxy region was proposed to possess three K homology-like RNA binding motifs and an SM protein-protein interaction motif (1, 62). Thus, the series of recombinant viruses used in this study (Table 1) will allow us to dissect the HSV-1 replication cycle and identify features needed for the prevention of apoptosis in the context of viral infection.

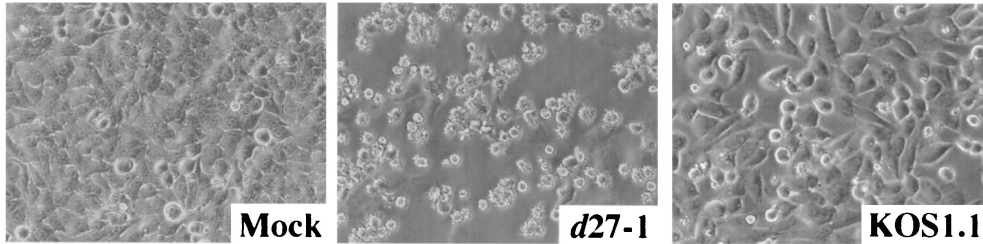
HEp-2 cells infected with ICP27 mutant viruses present apoptotic phenotypes. HEp-2 cells infected with an ICP27-null virus show features characteristic of apoptosis, including membrane blebbing, small irregularly shaped cells, and the generation of apoptotic bodies (1, 2; <http://www.mssm.edu/micro/blaho/webdata/maetaldns.shtml>). As an initial step in the current analysis, we determined whether cells infected with viruses carrying mutations of specific regions in ICP27 present similar apoptotic phenotypes. HEp-2 cells were infected with the series of mutant viruses shown in Table 1. At 24 h p.i., the infected cell morphologies were documented by phase-contrast microscopy, as described in Materials and Methods, and compared to those observed for wild-type- and *d27-1*-infected cells. The results (Fig. 2) were organized into two groups: ICP27 mutations affecting the amino domains and those affecting the carboxy domains.

Figure 2A shows that the infection of HEp-2 cells with the ICP27-null virus *d27-1* led to the appearance of small irregularly shaped cells. This result is identical to that obtained in our previous study in which HEp-2 cells were infected with another ICP27-null mutant virus, $\nu\text{BS}\Delta 27$ (1, 2). Smooth, rounded cells, exhibiting a classic HSV-1 cytopathic effect, were observed during wild-type KOS1.1 infection (Fig. 2A), as expected (1, 2). As with *d27-1*, nearly 100% of the cells infected with *d1-5* (Fig. 2B), *n263R*, or *n59R* (Fig. 2C) viruses presented apoptotic features. While a large number of cells showed small irregular shapes during *d1-2* (Fig. 2B), *n504R* and *n406R* (Fig. 2C), and M11, M15, and M16 (Fig. 2D) infections, a significant number of infected cells without any obvious apoptotic features could still be seen. Cells infected with *d2-3*, *d3-4*, *d4-5*, *d5-6*, or *d6-7* had little to no features characteristic of apoptotic cells (Fig. 2B) but look very similar to the cells after wild-type infection.

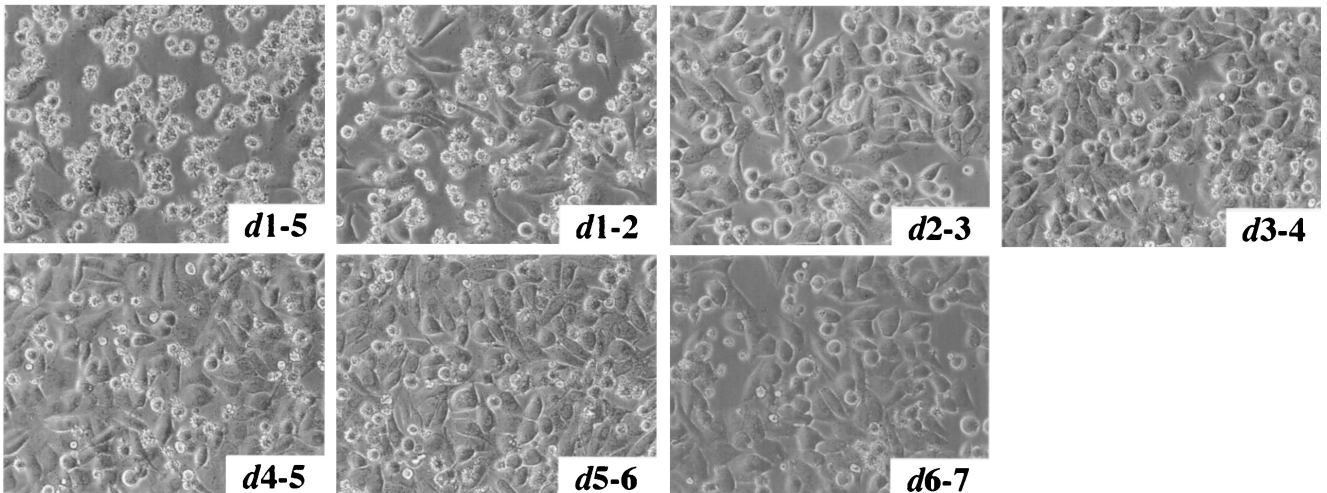
These results show that significant levels of apoptotic cells were generated with all mutant viruses containing either partial deletions or point mutations targeting the ICP27 carboxy domain. In the case of mutant viruses carrying deletions in the amino region, large numbers of apoptotic cells were only detected with *d1-5* and *d1-2*. These two viruses both contain deletions of the ICP27 acidic domain and NES (Fig. 1 and Table 1). The other ICP27 viruses with amino-domain deletions did not yield significant levels of apoptotic cells during infection. From these results, we conclude that regions in the amino portion of ICP27 other than the NES and acidic domain (Fig. 1) appear to be nonessential for its apoptosis prevention function, as several ICP27 N-terminal-mutant viruses show

Infected HEp-2 cell morphologies at 24 h p.i.

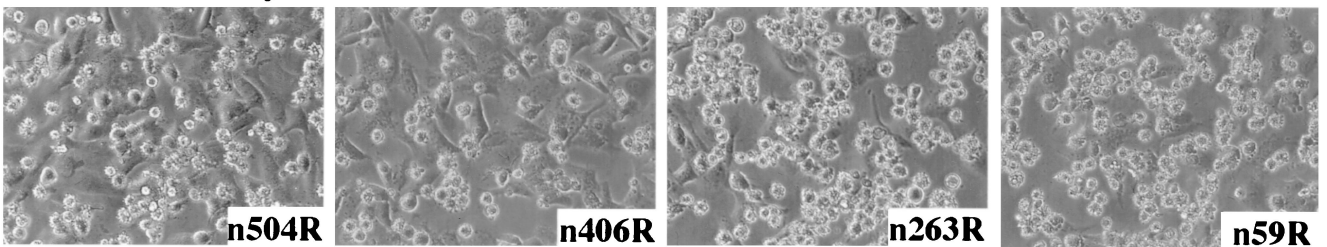
A. ICP27-null and wild type viruses



B. ICP27 amino-domain deletion viruses



C. ICP27 carboxy-domain deletion viruses



D. ICP27 carboxy-domain point mutation viruses

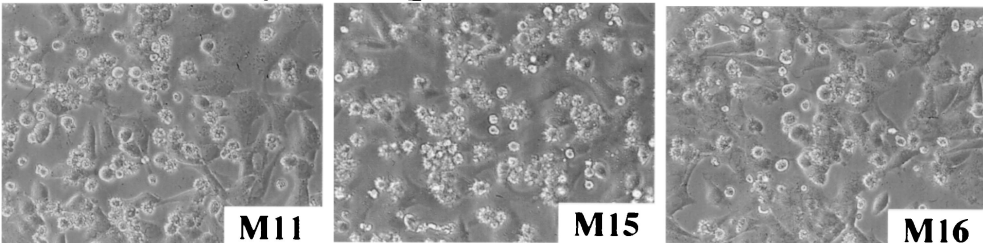


FIG. 2. Morphologies of HEp-2 cells infected with all viruses used in this study. Cells infected with *d27-1*, KOS1.1, and mock-infected virus (A) or viruses infected with ICP27 with an amino domain deletion (B), ICP27 with a carboxy domain deletion (C), and ICP27 with a carboxy domain point mutation (D) were observed at 24 h p.i. by phase-contrast microscopy (magnification, $\times 20$) as described in Materials and Methods.

infected-cell morphologies which are almost identical to that of wild-type KOS1.1 virus. While certain viruses are obviously apoptotic (e.g., *d1-2* and *d1-5*) and others are nonapoptotic (e.g., *d6-7*), certain other viruses (such as M11 and M16) appear to fall into a category of reduced apoptosis. This qualitative analysis suggests that our group of mutant viruses may be operationally defined as either apoptotic, partially apoptotic, or nonapoptotic. However, these gross cell morphology data are not sufficient to accurately quantitate the number of apoptotic cells during each infection.

Quantitation of apoptosis during ICP27 mutant virus infection of HEp-2 cells. The results in Fig. 2 indicate that infection of HEp-2 cells by various ICP27 mutant viruses can yield phenotypes identical to that observed with either KOS1.1 or *d27-1* infection. However, certain viruses also generate cell morphologies which, while possessing features consistent with apoptosis, are not as extreme as that observed with *d27-1*. Therefore, the goal of this set of experiments was to quantitate the number of apoptotic cells detected during infection with each one of the viruses used for Fig. 2. HEp-2 cells were mock infected or infected with each of our series of viruses (Table 1). At 15 h p.i., the cells were fixed and stained with Hoechst DNA dye prior to visualization by fluorescence microscopy, as described in Materials and Methods. As a control, the z-VAD-fmk general caspase inhibitor was added throughout the course of a *d27-1* infection. The percentage of total apoptotic cells detected was determined by counting the number of cells with condensed chromatin.

Figure 3A shows representative cell images of the following infections: mock, KOS1.1, *d27-1*, and *d27-1* plus the caspase inhibitor. Consistent with our previous findings (1), infection of HEp-2 cells with the ICP27-null virus *d27-1* resulted in almost all of the cells having condensed chromatin while little or no mock- and wild-type KOS1.1-infected cells had condensed chromatin. Cells infected with *d27-1* in the presence of the caspase inhibitor had nuclear morphologies which were similar to those of KOS1.1-infected cells. Based on these findings, we conclude that the apoptotic process which occurs during *d27-1* infection, resulting in chromatin condensation, proceeds through a caspase-dependent pathway. Since the z-VAD-fmk peptide is a general inhibitor, the identification of specific caspases was not addressed in this study.

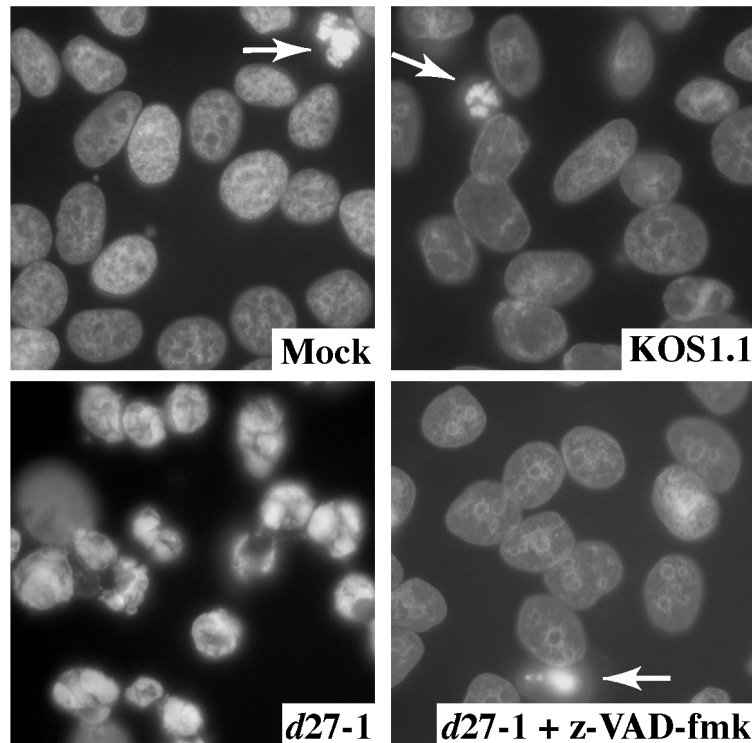
The results of our quantitation based on the number of cells with condensed chromatin are shown in Fig. 3B. Consistent with the results in Fig. 2, KOS1.1, *d2-3*, *d3-4*, *d4-5*, *d5-6*, and *d6-7* infection leads to less than 20% apoptotic cells, and these viruses are therefore considered nonapoptotic. Viruses M11, M16, *n504R*, and *n406R* generate between 31 and 42% apoptotic cells and are termed partially apoptotic. Infection with each of the remaining viruses produces greater than 50% apoptotic cells, and these viruses are therefore defined as apoptotic. As observed in Fig. 3A, the presence of the general caspase inhibitor during *d27-1* infection caused a decrease in apoptotic cells from approximately 90% (*d27-1* alone) to less than 5% (*d27-1* plus z-VAD-fmk). That this level of apoptosis was not reduced to zero could indicate that either the bioavailability of the peptide was not 100% or there was a minimal noncaspase-dependent process involved. Based on these results, we conclude that all of the viruses used in our study have the capacity to trigger apoptosis in HEp-2 cells. However, the

viruses differ in their ability to prevent the process from killing the cells. Accordingly, members of this group of viruses may be empirically defined as either nonapoptotic, partially apoptotic, or apoptotic.

Detection of cellular death factor processing following infection with ICP27 mutant viruses. The experiments for which results are shown in Fig. 2 and 3 focused on cell morphologies during infection. The goal of this series of experiments was to measure the extent of proteolytic processing of representative cellular proteins associated with the apoptotic program in HEp-2 cells. We previously showed that during vBSΔ27-induced apoptosis, certain cellular death factors such as PARP, DFF, and caspase-3 are processed (1). The possibility that wild type HSV-1 might degrade caspase-3 rather than activate it was excluded in experiments showing that full-length caspase-3 remains intact during productive HSV-1 infection when caspase inhibitors are present in the culture medium (1) (M. Aubert et al., data not shown). The processing of PARP, a 116,000-molecular-weight protein, generates an 85,000-molecular-weight product, and both forms were detected by the anti-PARP antibody used in this study (63, 67). Apoptosis-induced processing of DFF (molecular weight, 45,000) and caspase-3 (molecular weight, 32,000) resulted in the loss of reactivity with the anti-DFF and anti-caspase-3 antibodies. To analyze the processing of these death factors following infection with our series of viruses, HEp-2 cells were infected as for Fig. 2, whole extracts were made, and immunoblotting experiments were performed using anti-PARP, anti-caspase-3, and anti-DFF antibodies as described in Materials and Methods. To facilitate ease of comparison between each virus, relative amounts of processed PARP, unprocessed PARP, and caspase-3 were calculated. These values were determined after normalization to the amounts of α tubulin detected in each lane. The results showing PARP, caspase-3, and DFF processing are presented in Fig. 4.

The levels of the death factors detected at 24 h p.i. were largely consistent with the three groups defined by quantitating the percentages of cells showing chromatin condensation (Fig. 3). Apoptotic *d27-1*, *d1-5*, *d1-2*, M15, *n263R*, and *n59R* viruses showed significant PARP processing, as well as lower levels of caspase-3 and DFF compared to mock-infected cells (Fig. 4, compare lanes 2, 3, 4, 11, 13, 15, and 16 with lane 1). Infection with *d27-1*, *d1-5*, *d1-2*, M15, *n263R*, and *n59R* also generated large numbers of small, irregularly shaped cells, with a large percentage of cells with condensed chromatin (Fig. 2 and 3). In cells infected with viruses M11, M16, *n504R*, and *n406R*, processed PARP was detected at high levels but some amounts of unprocessed PARP were also observed (Fig. 4, lanes 10, 12, and 14). For M11, M16, *n504R*, and *n406R*, similar amounts of caspase-3 compared to that in KOS1.1-infected cells were detected while only slight reductions were seen with DFF (Fig. 4, compare lanes 6, 10, 12, and 14 with lanes 1 and 17). Although many cells infected with M11, M16, *n504R*, and *n406R* had small irregular shapes (Fig. 2), significant numbers without any obvious apoptotic features were also observed. In addition, M11, M16, *n504R*, and *n406R* generated between 31 and 42% apoptotic cells (Fig. 3) and were defined as partially apoptotic viruses. Finally, *d2-3*, *d3-4*, *d4-5*, *d5-6*, *d6-7*, and KOS1.1 correspond to the third group. In cells infected with these viruses, the relative amounts of full-length (116,000-molecular-weight)

A. Detection of apoptotic HSV-1-infected HEp-2 cells



B. Percentage of apoptotic HEp-2 cells after HSV-1 infection

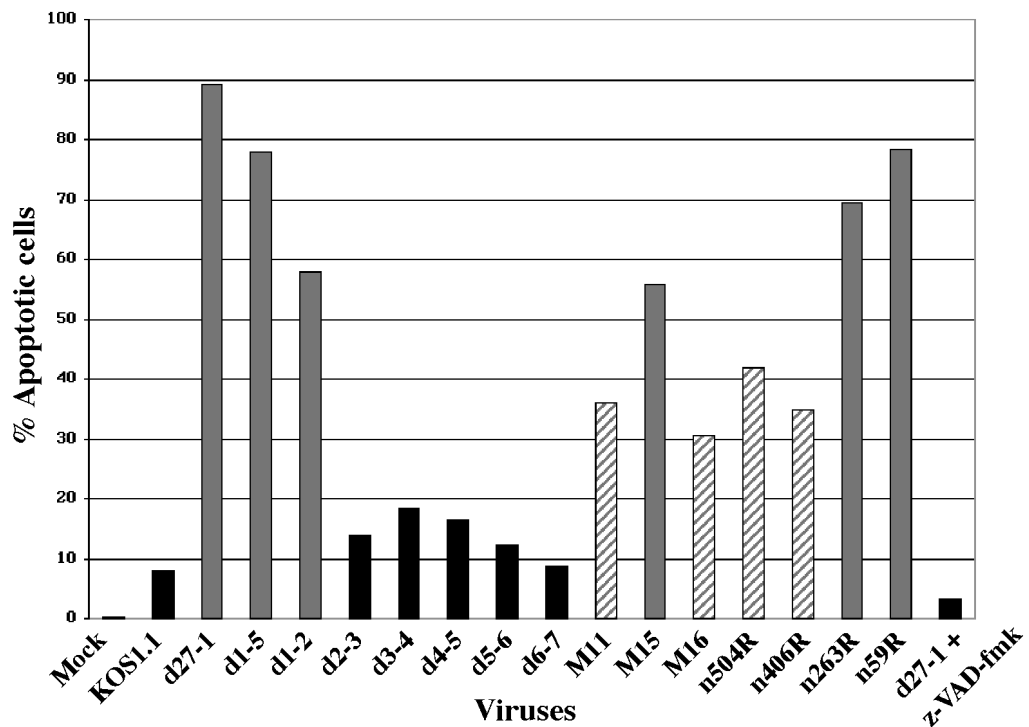


FIG. 3. Visualization (A) and quantitation (B) of apoptotic HSV-1-infected HEp-2 cells. Mock- and HSV-1-infected HEp-2 cells were fixed at 15 h p.i., stained with Hoechst 33258, and visualized by fluorescence microscopy (magnification, $\times 60$) as described in Materials and Methods. Panel A shows representative images of stained nuclei. *d27-1*-infected cells show classic condensed chromatin. The few apoptotic cells detected in mock-, KOS1.1-, and *d27-1*-infected cells in the presence of the general caspase inhibitory peptide (z-VAD-fmk) are marked by arrows. The percentage of apoptotic cells was determined by counting the number of infected cells with condensed chromatin. Gray, striped, and black histograms refer to apoptotic, partially apoptotic, and nonapoptotic viruses, respectively.

Cellular death factor processing at 24 hpi

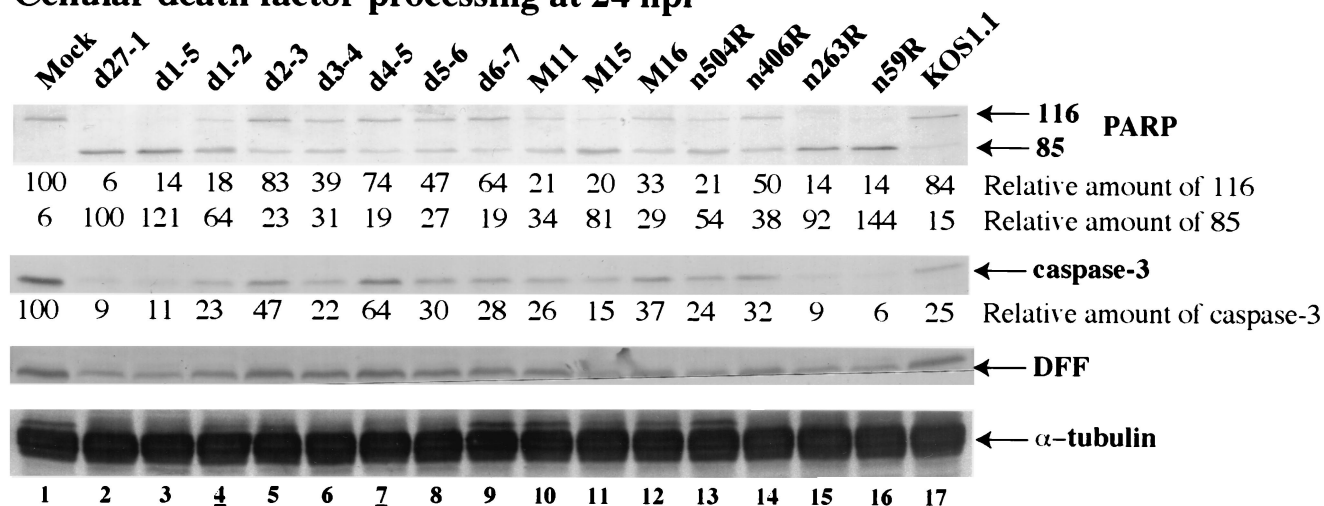


FIG. 4. Immunoblot detection of cellular death factor processing in infected HEp-2 cells. Whole-cell extracts prepared at 24 h p.i. were used for immunoblot analyses with anti-PARP, anti-DFF, anti-caspase-3, and anti- α tubulin antibodies. Amounts of full-length PARP, processed PARP, and caspase-3 were calculated relative to the amount of α tubulin as described in Materials and Methods. 116 and 85 refer to full-length and processed PARP, respectively. Lanes 4 and 7 are underlined to mark viruses analyzed in Fig. 7.

PARP versus processed (85,000-molecular-weight) PARP was either greater than two, as for *d2-3*, *d4-5*, *d6-7*, and KOS1.1 (Fig. 4, lanes 5, 7, 9, and 17) or between one and two, as for *d3-4* and *d5-6* (Fig. 4, lanes 6 and 8). The relative amount of caspase-3 was either similar to or higher than in KOS1.1, while the amount of DFF observed was similar (Fig. 4, compare lanes 5 and 7 through 9 with lane 17). Infection by *d2-3*, *d3-4*, *d4-5*, *d5-6*, *d6-7*, and KOS1.1 produce little if any morphological sign of apoptosis (Fig. 2 and 3), and these viruses were defined as nonapoptotic.

These biochemical results confirm our previous microscopic observations (Fig. 2 and 3) that all cells infected with the ICP27 carboxy-domain-mutant viruses showed extensive signs of apoptosis while only the cells infected with *d1-2* and *d1-5* amino-domain-deletion viruses presented biochemical features of apoptosis which were significantly above the background level observed with wild-type KOS1.1. From these results we can conclude that ICP27 possesses functional regions which are nonessential for apoptosis prevention, e.g., the RGG box RNA binding motif. In addition, for the mutants which are able to block apoptosis the degree of protection varies depending on the nature of the mutation. Thus, the *d1-2* virus represents a group of viruses which cannot block apoptosis while *n406R* represents a group which shows partial prevention.

Viruses carrying mutations in ICP27's N-terminal acidic domain or the activation/repression domain are impaired for growth in Vero cells. The prior series of experiments demonstrated that viruses containing ICP27 mutations can be defined as either apoptotic, partially apoptotic, or nonapoptotic based on their properties observed during infection of HEp-2 cells. In order for us to use these viruses as tools to fully understand the aspects of HSV-1 infection which are required for the apoptotic prevention process, the goal of our remaining experiments was to compare the capacities of the viruses to block apoptosis with their abilities to productively replicate, synthesize viral

DNA, and accumulate viral proteins. Traditionally, ICP27 functions have been assessed using Vero cells. Previously, we showed that the vBS Δ 27 ICP27-null virus does not induce apoptosis in Vero cells (1). We suggested that this may be because Vero cells have lost their ability to efficiently activate proapoptotic pathways in response to HSV-1 infection. In this portion of the study, we assessed the ability of our viruses to replicate under conditions in which apoptotic prevention functions are not required. The titers of each virus in Vero and V27 (ICP27-expressing Vero) cells were measured (Table 2). These data were compared (Table 2) to the number of apoptotic cells (Fig. 3) and the extent of PARP processing by comparing the relative amounts of processed and unprocessed PARP (Fig. 4).

While all of the mutant viruses have titers which are very similar to those of wild-type KOS1.1 in V27 cells, they can be separated into three groups based on their ability to grow in Vero cells. The first group, containing *d2-3*, *d3-4*, *d5-6*, and *d6-7*, had similar titers on both Vero and V27 cells. The percentage of apoptotic cells (9 to 18%) and the calculated percentages of PARP processing (30 to 54%) for each of these viruses were only slightly greater than those of KOS1.1 (8 and 21%, respectively). The second group, containing *d1-2* and *d4-5*, had titers on Vero cells which were reduced by 3 to 4 logs compared to KOS1.1. *d1-2* was apoptotic (58% apoptotic cells and 84% PARP processing), while *d4-5* was nonapoptotic (17% apoptotic cells and 21% PARP processing). Finally, the third group is formed by *d27-1*, *d1-5*, M11, M15, M16, *n504R*, *n406R*, *n263R*, and *n59R*, which were unable to grow on Vero cells (titers from $<2 \times 10^2$ to 4.2×10^3). All of these last viruses were either apoptotic or partially apoptotic (Table 2).

M16 and *n406R* are of particular interest since they are highly defective for growth in Vero cells, but they show low (but still significant) percentages of apoptosis (31 and 35% apoptotic cells and 58 and 53% PARP processing, respectively). In contrast, the partially apoptotic M11 virus had 36%

Viral DNA replication in ICP27 mutant-infected HEP-2 cells

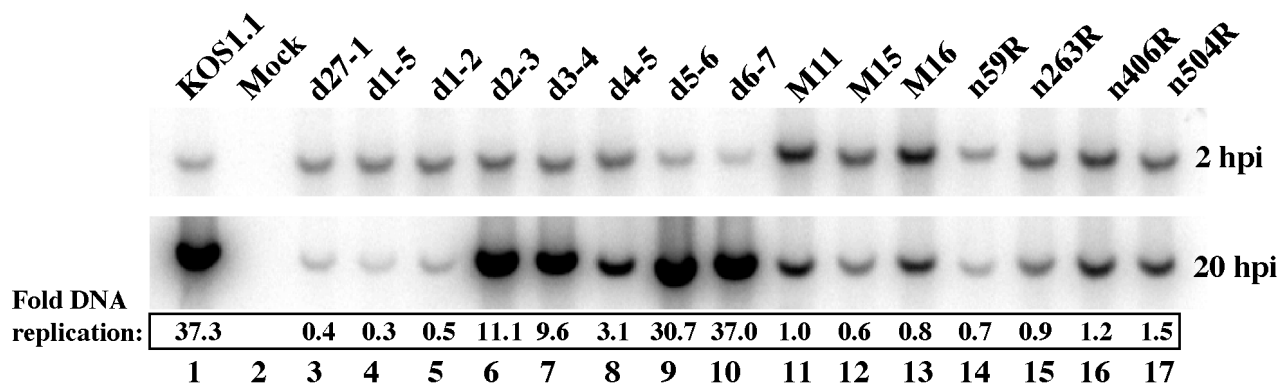


FIG. 5. Autoradiographic images of viral DNA. Total DNA was isolated from infected HEP-2 cells at 2 and 20 h p.i., digested with *Pst*I, separated in an agarose gel, transferred to a nylon membrane, and hybridized with a radioactive probe derived from a portion of the HSV-1 U_L44 gene, prior to autoradiography, as described in Materials and Methods. Amounts of DNA were quantitated using a phosphorimager, and values of fold-DNA replication were calculated by dividing the radioactive signal at 20 h p.i. (replicated DNA) by the signal at 2 h p.i. (input DNA).

apoptotic cells but 71% PARP processing. This feature of M11, that the number of apoptotic cells is low while the amount of PARP processing is somewhat high, is similar to that observed with the *d3-4* (18% apoptotic cells and 54% PARP processing), *d5-6* (12% apoptotic cells and 46% PARP processing), and *d6-7* (9% apoptotic cells and 31% PARP processing) viruses, which grew equally well on Vero and V27 cells and which we have defined as nonapoptotic.

These results confirm and extend previous results (summarized in Table 1) showing that ICP27-defective viruses containing mutations in or of (i) the activation/repression domain, (ii) the first third of the amino-terminal region containing the acidic domain, and (iii) the sequences involved in nuclear localization and RNA binding (NLS, NuLS, and RGG) are significantly impaired for growth in noncomplementing Vero cells. However, not all viruses which are impaired for efficient viral growth in Vero cells present apoptotic features in HEP-2 cells. This phenomenon is best observed with *d4-5*, whose mutation affects ICP27's NuLS and RGG box. The *d4-5* virus is nonapoptotic, but its growth efficiency in Vero cells is reduced by almost 3 logs compared to that of KOS1.1. This finding indicates that certain ICP27 functions which are necessary for efficient productive replication may be separable from the antiapoptotic activity. Specifically, ICP27's NuLS and RGG box are needed for efficient replication but do not appear to be required for apoptosis prevention.

Viral DNA synthesis in ICP27 mutant-infected HEP-2 cells.

The goal of our final series of experiments was to determine as precisely as possible the feature of HSV-1 replication that correlates with the prevention of apoptosis in infected HEP-2 cells. The results presented in Table 2 show a comparison of the antiapoptotic potentials of our series of viruses with their abilities to efficiently replicate in Vero cells. Previously (48–50), the abilities of a subset of these viruses to synthesize their genomic DNA in Vero cells were determined (results summarized in Table 1). While DNA replication is a central event in the HSV-1 lytic cycle, ICP27 is not absolutely essential for this process in Vero cells (49). Viruses *d27-1*, *d1-2*, *n406R*, *n263R*,

and *n59R* are defective for DNA replication in Vero cells, but M11, M15, M16, and *n504R* show levels of DNA replication that are comparable to that of the wild-type virus. Thus, it was of interest to measure the levels of viral DNA replication for each virus in HEP-2 cells to see if this process correlates with apoptosis prevention. At 2 and 20 h p.i., total infected cell DNA was isolated and digested with *Pst*I. DNA hybridization was performed using a radioactive probe derived from the HSV-1 U_L44 gene (gC), and the amounts of viral DNA detected at the two time points were compared using a phosphorimager as described in Materials and Methods. For each infection, the radioactive signal at 20 h p.i. (replicated DNA) was divided by the signal at 2 h p.i. (input DNA) to generate values of fold DNA replication. The results (Fig. 5) were as follows.

The data for KOS1.1 and *d27-1* viruses (37.3- and 0.4-fold DNA replication, respectively) indicate that ICP27 is essential for significant viral DNA replication in HEP-2 cells. The remaining mutant viruses appear to fall into three categories with respect to their ability to replicate their DNA. The first group, containing the *d5-6* and *d6-7* viruses, had wild-type levels (30.7- to 37.3-fold) of DNA synthesis (Fig. 5, lanes 1, 9, and 10). The second group, formed by the *d2-3*, *d3-4*, and *d4-5* viruses, showed significant viral DNA replication (3.1- to 11.1-fold) but at reduced levels compared to KOS1.1 (Fig. 5, compare lanes 6 to 8 with lane 1). All of the viruses in these first two groups were defined previously as nonapoptotic. The third group contains the remaining viruses, *d1-5*, *d1-2*, M11, M15, M16, *n504R*, *n406R*, *n263R*, and *n59R*, and showed very little to no DNA synthesis. These viruses had between 0.3- and 1.5-fold DNA replication by 20 h p.i., which means that they were nearly as defective as the *d27-1* virus (Fig. 5, lanes 3 to 5 and 11 to 17). This group of viruses contains all of the apoptotic (*d27-1*, *d1-5*, *d1-2*, M15, *n263R*, and *n59R*) and partially apoptotic (M11, M16, *n504R*, and *n406R*) viruses. These findings are in contrast to results obtained in Vero cells (Table 1), in which the M11, M15, M16, and *n504R* viruses replicate their DNA at wild-type levels. This discrepancy may be due, at least partially, to the fact that apoptosis occurring in M11-, M15-,

Viral protein accumulation at 24 hpi

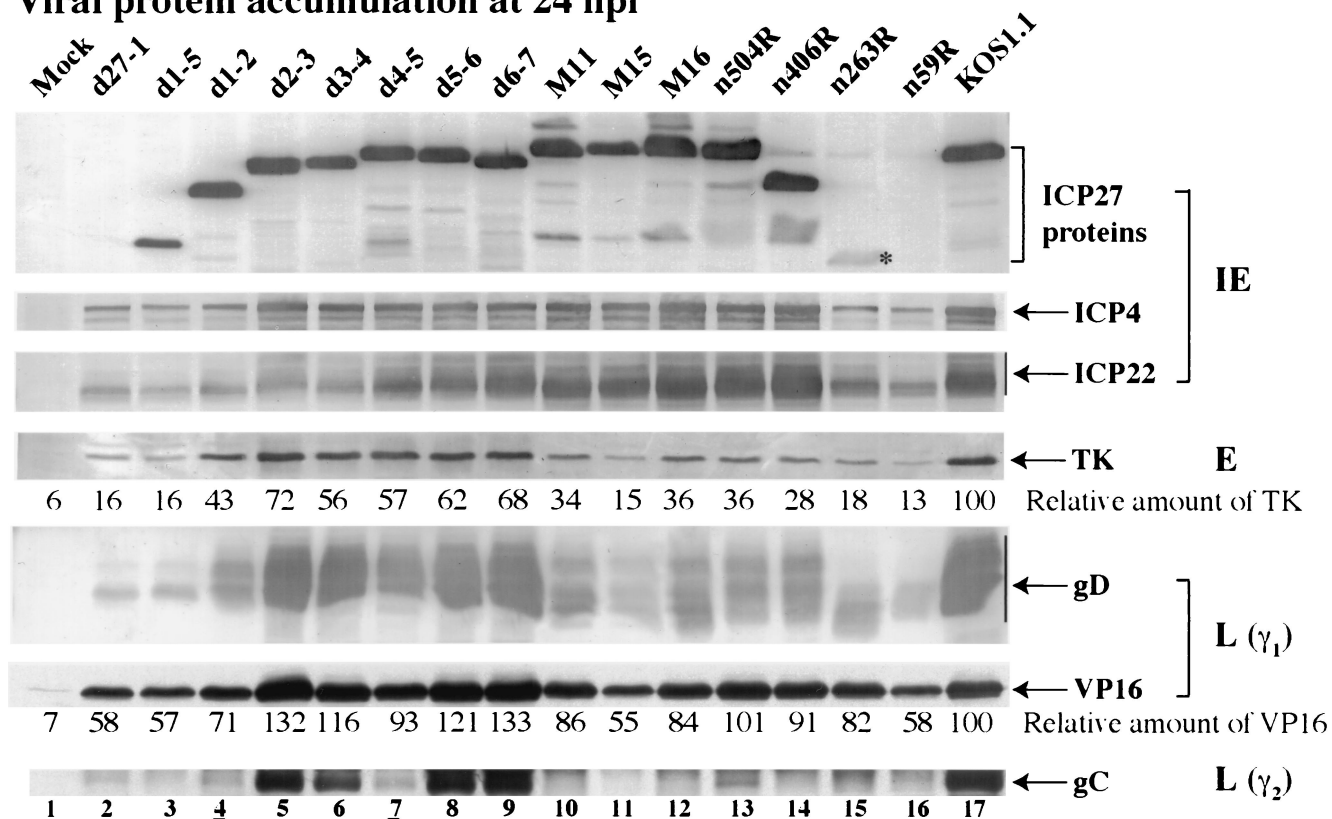


FIG. 6. Immunoblot detection of viral protein accumulation in infected HEp-2 cells. Whole-cell extracts prepared at 24 h p.i. were used for immunoblot analyses with anti-ICP27, anti-ICP4, and anti-ICP22 (IE proteins), anti-TK (E protein), anti-VP16 and anti-gD (L proteins, γ_1), and anti-gC (L protein, γ_2) antibodies. Relative amounts of TK and VP16 were normalized to the amount of α tubulin and calculated as described in Materials and Methods. An asterisk marks *n263R* ICP27 protein since its accumulation is at low levels. Lanes 4 and 7 are underlined to mark viruses analyzed in Fig. 7.

M16-, and *n504R*-infected HEp-2 cells would be expected to limit viral DNA replication.

The above results suggest that viruses which are able to efficiently prevent apoptosis (nonapoptotic) in HEp-2 cells proceed to the DNA replication stage of viral infection. Additionally, our findings suggest that it is not the magnitude of the viral DNA synthesis which is important for apoptosis prevention but rather the entry of the virus into this specific stage of the productive cycle. This model is based on the observation that while the values of fold DNA replication for KOS1.1, *d2-3*, *d3-4*, *d4-5*, *d5-6*, and *d6-7* range from 37.3 down to 3.1, all of these viruses prevent apoptosis by similar degrees (Fig. 3 and Table 2). To further investigate this hypothesis, we next focused on determining the levels of accumulation of viral proteins representative of the different classes of viral gene expression.

Accumulations of TK, VP16, and gD but not gC, ICP22, or ICP4 correlate with prevention of apoptosis during HSV-1 infection. To assess the progression of viral replication, each infected cell sample for which data are presented in Fig. 4 was tested for the accumulation of representative viral proteins at 24 h p.i. Immunoblotting analyses were performed using antibodies specific for ICP27, ICP4, ICP22, TK, VP16, gD, and gC, and the results are presented in Fig. 6.

Levels of the IE ICP27, ICP4, and ICP22 proteins were examined first. As expected (48), no ICP27 was detected with *d27-1* and *n59R*, while low levels were seen with *n263R*. Large amounts of ICP27 were detected with all other viruses. The lowest ICP4 levels were seen in *d27-1*-, *d1-5*-, *d1-2*-, *n263R*-, and *n59R*-infected cells (Fig. 6, compare lanes 2 to 4, 15, and 16 with lane 17). Similar amounts of ICP4 were detected with all other viruses compared with wild-type KOS1.1 levels. ICP22 accumulation varied from (i) very low levels for viruses *d27-1*, *d1-5*, *d1-2*, *d2-3*, *d3-4*, *n263R*, and *n59R* (Fig. 6, lanes 2 to 6, 15, and 26), (ii) slightly reduced levels for *d4-5*, *d5-6*, *d6-7*, M11, and M15 (Fig. 6, compare lanes 7 to 11 with lane 17), to (iii) amounts of ICP22 similar to those in KOS1.1-infected cells for M16, *n504R*, and *n406R* (Fig. 6, compare lanes 12 and 13 with lane 17). This analysis shows that viruses which have the highest potential to produce apoptosis (e.g., *d27-1*, *d1-5*, *d1-2*, *n263R*, and *n59R*) had the lowest levels of ICP4, consistent with our original observations obtained with the ICP27-null virus vBSA27 (1). However, we detected essentially wild-type levels of ICP4 with M11, M15, M16, *n504R*, and *n406R* viruses, suggesting that the presence of ICP4 is not sufficient to block apoptosis. Apoptosis prevention also did not correlate with ICP22 production as low levels of ICP22 were seen in both

viruses that could (*d2-3* and *d3-4*) and could not (*d27-1*, *d1-5*, *d1-2*, *n263R*, and *n59R*) prevent apoptosis.

Next, we tested for accumulation of the TK protein, a representative early viral protein. Very little TK (13 to 18%) was observed (Fig. 6, lanes 2, 3, 11, 15, and 16) with viruses *d27-1*, *d1-5*, M15, *n263R*, and *n59R* compared to that observed with KOS1.1 (100%). Viruses *d1-2*, M11, M16, *n504R*, and *n406R* produced lower amounts of TK than KOS1.1 (between 28 and 43%) (Fig. 6, lanes 4, 6, 10, 12 to 14, and 17). Finally, in cells infected with *d2-3*, *d3-4*, *d4-5*, *d5-6*, and *d6-7* reduced amounts of TK (56 to 72%) were detected (Fig. 6, compare lanes 5 to 9 with lane 17). Thus, viruses which were able to synthesize significant amounts of TK (E protein) could also block apoptosis. This finding corroborates our previous conclusion that infected cell protein produced during the transition from the IE to E phases (between 3 and 6 h p.i.) is required for apoptosis prevention (2).

The last set of viral proteins analyzed were the late proteins VP16 (γ_1), gD (γ_1), and gC (γ_2); gC belongs to the class of "true late" proteins whose synthesis requires viral DNA synthesis. Compared to KOS1.1-infected cells, the amounts of VP16 detected in cells infected with mutant viruses were either (i) lower (from 55 to 71%), as for *d27-1*, *d1-5*, *d1-2*, M15, and *n59R* (Fig. 6, compare lanes 2 to 4, 11, and 16 with lane 17), (ii) slightly lower to similar, as for *d4-5*, M11, M16, *n406R*, and *n263R* (Fig. 6, compare lanes 10, 12, 14, and 15 with lane 17), or (iii) higher, as for the remaining viruses (Fig. 6, compare lanes 5 to 9 and 13 with lane 17). Concerning gD accumulation, high amounts were detected for KOS1.1, *d2-3*, *d3-4*, *d4-5*, *d5-6*, and *d6-7* viruses (Fig. 6, lanes 5 to 9 and 17). For the remaining viruses, either low (M11, M16, *n504R*, and *n406R*) or very low (*d1-2*, M15, *n263R*, and *n59R*) amounts of gD were observed (Fig. 6, lanes 4 and 10 to 16). Since these accumulations were measured at 24 h p.i., we do not know whether input virus contributes the levels of VP16, gD, and gC detected. In general, the patterns of accumulations of VP16 and gD followed that of TK, except that the control amount of VP16 in KOS1.1 was somewhat lower than that observed with several mutant viruses. Since our calculations of the amounts of VP16 were relative to the KOS1.1 amount, values greater than 100 were produced. It was expected that VP16, gD, and TK would be observed at similar times since gD and VP16 can be considered leaky-late viral proteins.

In the case of the gC protein, only the *d2-3*, *d3-4*, *d5-6*, and *d6-7* viruses produced protein levels similar to those of the wild-type virus (Fig. 6, compare lanes 5, 6, 8, and 9 with lane 17). Each of these viruses is considered nonapoptotic, and each synthesizes viral DNA in infected HEP-2 cells (Fig. 5). Very little to no gC was detected with the remaining 11 viruses. As expected, these viruses which did not produce gC also did not synthesize viral DNA (Fig. 5). The one exception in the group is the nonapoptotic *d4-5* virus, which synthesizes DNA in HEP-2 cells, albeit at a low level, but does not accumulate gC. One possible explanation for this finding is that the level of DNA synthesis during *d4-5* infection is simply not sufficient for optimal true late gene expression. This finding suggests that expression of true late genes is not required for apoptosis prevention.

To summarize the experiments discussed in this section, we examined a large number of ICP27 mutant viruses for the

synthesis of selected representative viral gene products. Since most of the mutants produce levels of ICP27 protein indistinguishable from that in KOS1.1-infected cells, their phenotypes are likely due to the loss of specific functional regions and not simply a result of lower amounts of this α regulatory protein. Comparison of the results of Fig. 6 with those in Fig. 2 to 4 demonstrates that a correlation exists between the accumulation of TK, gD, and VP16 and the extent of apoptotic features in infected HEP-2 cells. In contrast, the abilities of the various mutants to prevent apoptosis do not appear to correlate with synthesis of either ICP4, ICP22, or gC. These results suggest that prevention of apoptosis by ICP27 may be due to its ability to induce the optimal synthesis of early or leaky-late viral gene products.

Results obtained with the nonapoptotic *d4-5* virus support a role for early/leaky-late gene products in apoptosis prevention. Of the five nonapoptotic mutant viruses, *d2-3*, *d3-4*, *d5-6*, and *d6-7* behave essentially the same as wild-type KOS1.1 in all of the assays we have used. The *d4-5* virus represents one of the more interesting viruses in the nonapoptotic group. While all of these five viruses prevent apoptosis by similar degrees (Fig. 3 and Table 2), the value of fold DNA replication for *d4-5* is the lowest in the group (Fig. 5). This observation suggested that it is not the magnitude of the viral DNA synthesis which is important for apoptosis prevention but rather the entry of the virus into a specific stage of the productive cycle.

The results in Fig. 2 to 5 and Table 2 were generated from single viral isolates. For example, *d4-5a* and *d1-2a* were used in all of the previous experiments. To confirm the observed cellular protein processing and viral protein accumulations with the nonapoptotic *d4-5* virus, we repeated the previous experiments using two independent plaque isolates (a and b). Two isolates of the apoptotic *d1-2* virus were included in this experiment as a control along with the *d27-1* and KOS1.1 viruses, as this virus possesses a growth defect in Vero cells which is comparable to that of *d4-5* (Table 2). As expected (Fig. 2), essentially all cells showed features characteristic of apoptosis when infected with isolates a and b of the *d1-2* virus (Fig. 7A). In this experiment, isolate *d1-2b* had a slightly larger number of apoptotic cells than *d1-2a*. No apoptotic features were observed for *d4-5a*- and *d4-5b*-infected cells, which appeared to be very similar to KOS1.1-infected cells (Fig. 7A).

An immunoblotting analysis (Fig. 7B) was also performed using the cells shown in Fig. 7A to detect the processing of PARP and caspase-3 proteins at 24 h p.i. High levels of processed PARP and very low amounts of caspase-3 were detected in *d27-1*-, *d1-2a*-, and *d1-2b*-infected cells (Fig. 7B, lanes 2 to 4). In this experiment, the extent of processing differed slightly between the three different infected cell populations but it corresponded well with the number of infected cells presenting apoptotic morphologies (Fig. 7A), such that the order was *d27-1*>*d1-2b*>*d1-2a*. The results with *d4-5a* and *d4-5b* were surprising (but comparable to that in Fig. 4, lane 7) because the extents of PARP and caspase-3 processing were less than for the wild-type KOS1.1 control (Fig. 7B, compare lanes 5 and 6 with 7). We have observed this phenomenon previously using a virus which contains a deletion of the virion host shutoff (*vhs*) gene (U_L41) and concluded that *vhs* may function in the induction of apoptosis during HSV-1 infection (2).

When we tested for the accumulation of specific viral pro-

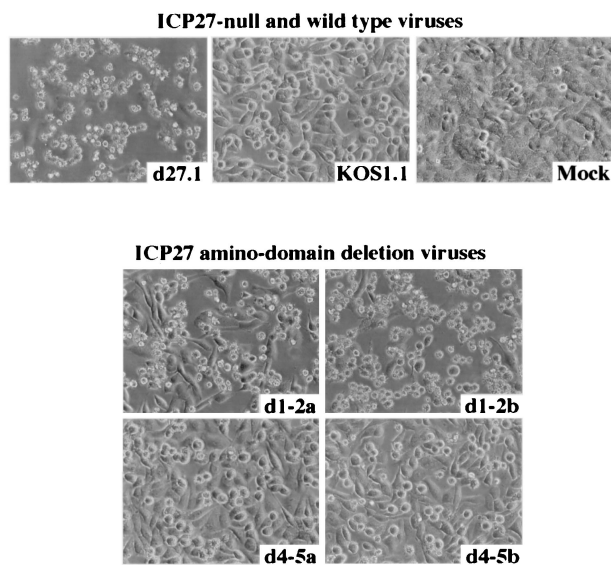
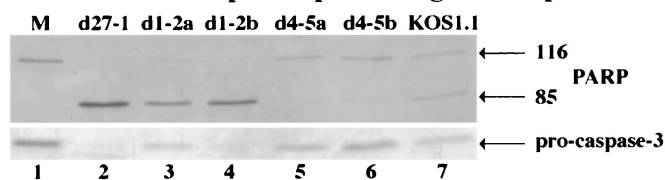
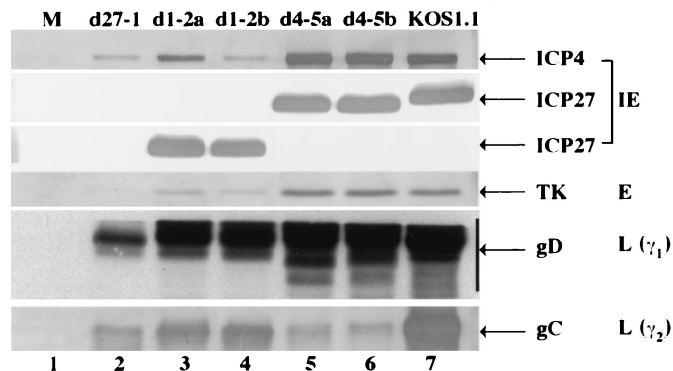
A. Infected HEp-2 cell morphologies at 24 h p.i.**B. PARP and caspase-3 processing at 24 h p.i.****C. Viral protein accumulation at 24 h p.i.**

FIG. 7. Morphologies (A) and immunoblot detection of PARP and caspase-3 processing (B) and viral protein accumulation (C) in *d1-2*- and *d4-5*-infected HEp-2 cells. Cells infected with *d27-1*, KOS1.1, *d1-2* (isolate a or b), and *d4-5* (isolate a or b) viruses and mock-infected cells were observed at 24 h p.i. by phase-contrast microscopy (magnification, $\times 20$). Whole-cell extracts prepared at 24 h p.i. were used for immunoblot analyses with anti-PARP and anti-caspase-3 antibodies or with anti-ICP27, anti-ICP4 (IE proteins), anti-TK (E protein), anti-gD (L protein, γ_1), and anti-gC (L protein, γ_2) antibodies as described in Materials and Methods. 116 and 85 refer to full-length and processed PARP, respectively.

teins (Fig. 7C), we observed high levels of ICP27 with all viruses except *d27-1*. ICP4, TK, and gD levels were the same with *d4-5a*, *d4-5b*, and KOS1.1 and reduced with *d27-1*, *d1-2a*, and *d1-2b*. The results with *d27-1* and *d1-2* are consistent with our earlier finding that the most highly apoptotic viruses have reductions in the accumulation of ICP4 (Fig. 6). All viruses had reduced amounts of gC compared to KOS1.1. gC levels obtained with *d27-1*, *d4-5a*, and *d4-5b* were essentially the same and lower than those obtained with both *d1-2a* and *d1-2b*. While the *d1-2b* infection appeared to have been slightly more efficient in inducing apoptosis than that with *d1-2a* in this experiment, the cell morphologies and protein accumulation patterns were generally the same. These results indicate that the *d1-2* and *d4-5* phenotypes are consistent between independent plaque isolates. Furthermore, they confirm our finding that the synthesis of wild-type levels of gC, and likely other true late gene products, is not required for the prevention of apoptosis.

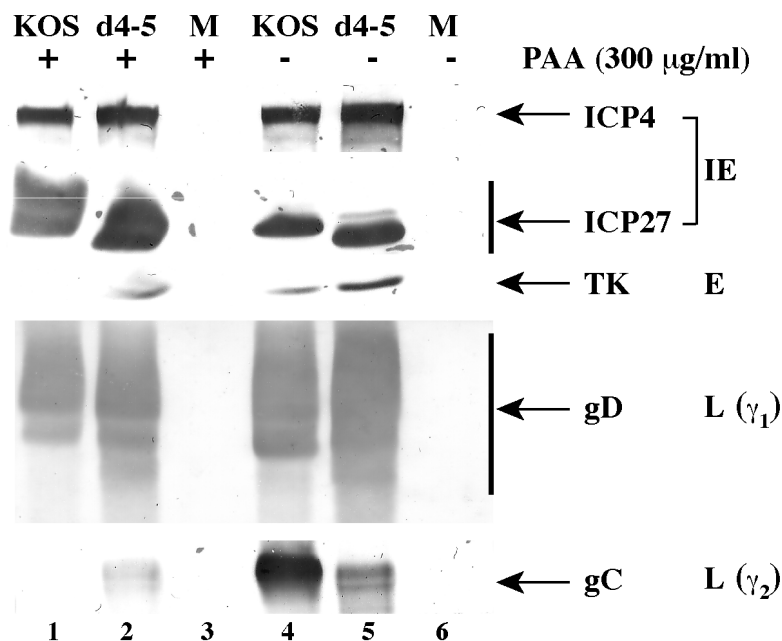
These results suggest that the synthesis of early/leaky-late viral proteins are involved in apoptosis prevention, inasmuch as *d4-5* produces wild type levels of TK, VP16, and gD with little to no gC and it is a nonapoptotic virus. One intriguing observation is that cells infected with the recombinant virus *d4-5*, which contains a deletion of the ICP27 RGG box, seem to undergo less apoptosis than wild-type KOS1.1-infected cells. The basis of this phenomenon remains to be determined.

Viral DNA synthesis and the production of true late gene products are not required for prevention of apoptosis in infected HEp-2 cells. The results in Fig. 5 indicate that apoptosis prevention by HSV-1 correlates with the infection proceeding

to the viral DNA synthesis stage, but it is not necessary to generate wild-type levels of viral DNA replication. Furthermore, the results in Fig. 6 and 7 suggest that true late (γ_2) viral proteins are not required for the prevention activity. Since the expression of γ_2 genes is absolutely dependent on viral DNA synthesis, the goal of this experiment was to determine whether HSV-1 could block apoptosis under infection conditions in which the process of viral DNA synthesis was specifically inhibited. In this experimental situation, productive viral replication will proceed to the point where the factors required for viral DNA replication are produced but where the polymerase activity is blocked. HEp-2 cells were mock, KOS1.1, and *d4-5* infected in the presence or absence of 300 μg of phosphonoacetic acid (PAA) per ml. This amount of PAA was previously shown to be sufficient to completely block HSV-1(F) DNA synthesis in infected human cells (5). Whole-cell extracts were prepared at 24 h p.i. and used for immunoblot analyses with anti-PARP, -caspase-3, -ICP27, -ICP4, -TK, -gD, and -gC antibodies (Fig. 8).

The accumulations of the viral ICP4, ICP27, TK, and gD proteins were the same for KOS1.1 and *d4-5* with or without the drug. There were less of these proteins detected with KOS1.1 than with *d4-5* under both infection conditions (Fig. 8A, compare lanes 1 and 2 with 5 and 6). As expected, the amount of gC was less with *d4-5* than with KOS1.1 in the absence of PAA (Fig. 8A, compare lanes 5 and 4). In the presence of PAA, little if any gC was detected with both viruses (Fig. 8A, lanes 1 and 2). These results were anticipated and indicate that the drug effectively prohibits viral DNA synthesis during infection. The slight amount of gC produced by *d4-5* did

A. Accumulation of viral proteins in infected HEp-2 cells



B. PARP and caspase-3 processing in infected HEp-2 cells

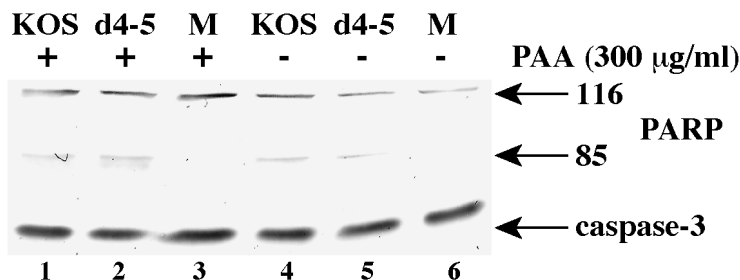


FIG. 8. Viral protein accumulation (A) and immunoblot detection of cellular death factor processing (B) in mock (M)-, KOS1.1-, and *d4-5*-infected HEp-2 cells in the presence (+) or absence (-) of PAA (300 µg/ml). Whole-cell extracts prepared at 24 h p.i. were used for immunoblot analyses with anti-PARP and anti-caspase-3 antibodies or with anti-ICP27 and anti-ICP4 (IE proteins), anti-TK (E protein), anti-gD (L protein, γ_1), and anti-gC (L protein, γ_2) antibodies as described in Materials and Methods. 116 and 85 refer to full-length and processed PARP, respectively.

not significantly change in the presence or absence of PAA. Identical results were also obtained using 5-bromodeoxyuridine (Aubert et al., data not shown). In addition, slight reductions in ICP4, ICP27, TK, and gD were observed when either PAA (Fig. 8) or 5-bromodeoxyuridine (Aubert et al., data not shown) was added. Taken together, these findings suggest that the minimal amount of gC detected in *d4-5*-infected cells appears to be independent of viral DNA synthesis. The data in Fig. 8B show that only slight amounts of PARP and caspase-3 processing were detected with KOS1.1 and *d4-5* in the presence and absence of PAA (compare lanes 1 and 2 with 5 and 6). The apparent reduction in the amount of mock protein likely represents minor experiment-to-experiment variation. Taking these observations together, we conclude that neither viral DNA synthesis nor the production of true late viral pro-

teins is required for the prevention of apoptosis in infected HEp-2 cells.

DISCUSSION

We previously reported that a recombinant HSV-1 containing a complete deletion of the ICP27 gene was able to induce but not prevent apoptosis in human HEp-2 cells during infection (1). At least two models exist to explain these findings. (i) ICP27 itself may directly inhibit apoptosis. (ii) Alternatively, or additionally, ICP27 may induce the expression of other viral or cellular “preventers” of apoptosis. The goal of this project was to use a series of recombinant ICP27 mutant viruses to determine which features of the HSV-1 replication cycle are required for its inhibitory activity. In addition, these mutant

viruses can provide novel information on the regulatory functions of ICP27 in infected human HEp-2 cells. The significant findings of our study can be summarized as follows.

Significant findings. (i) Recombinant ICP27 mutant viruses exhibit apoptotic, partially apoptotic, or nonapoptotic phenotypes in HEp-2 cells. Since ICP27-null viruses are completely unable to prevent apoptosis during infection, it was important to quantitatively determine whether various recombinant viruses mutated in specific regions of ICP27 could inhibit the process. To attain this goal, it was necessary for us to develop assays which would allow us to accurately quantitate the extent of this complex biological process. The phenomenon of apoptosis in human cells was originally defined in structural terms (29, 68). The defining features of the process are chromatin condensation (pyknosis), fragmentation of nuclei (karyorrhexis), specific nucleosomal laddering, membrane blebbing, and the formation of apoptotic bodies. Apoptosis is currently recognized as resulting from regulated proteolysis (11, 17, 28, 31, 39, 54). When developing assays for measuring apoptosis during HSV-1 infection it was necessary to avoid potentially misleading results due to consequences of viral replication, such as the generation of substrates for terminal deoxynucleotidyl transferase (i.e., TUNEL) by random nicking of cellular DNA. For this reason we chose three complementary techniques based on changes in endogenous cellular components. We previously reported that microscopic inspection of ICP27-null-virus-infected HEp-2 cells reveals cell shrinkage, membrane blebbing, and the formation of apoptotic bodies (1). This technique was used to make preliminary classifications of the viruses. These original assignments were confirmed by quantitation of cells presenting condensed chromatin following infection: nonapoptotic, below 20%; partially apoptotic, between 20 and 50%; apoptotic, greater than 50%. Finally, our placement of the viruses in each group was substantiated by assays designed to detect the endogenous levels of cellular death factor processing.

(ii) Apoptosis prevention requires that HSV-1 infection proceed to the stage in which viral DNA replication takes place. Our experiments demonstrate that the viruses defined as nonapoptotic are those which are able to synthesize their DNA to some extent in HEp-2 cells. However, since there is at least a 10-fold variation in the amounts of the DNA replicated by these viruses, it appears that the magnitude of DNA synthesis is not a major determinant of apoptosis prevention. The more likely possibility is that apoptosis prevention requires that HSV-1 infection proceed to a point at which the factors necessary for viral DNA replication have accumulated. To confirm this hypothesis, we performed infections with the nonapoptotic KOS1.1 and *d4-5* viruses in the presence of the DNA synthesis inhibitor PAA. The absence of apoptosis under these conditions confirmed that it is not the act of viral DNA synthesis itself which is required for apoptosis prevention. Since the expression of viral γ_2 genes is absolutely dependent on viral DNA synthesis, the results also demonstrated that the accumulation of true late gene products is not required for the prevention of apoptosis.

(iii) Accumulation of viral early and leaky-late proteins correlates with prevention of apoptosis. Having grouped all viruses based on their apoptotic potentials, we attempted to correlate the apoptotic phenotypes of the viruses with their

abilities to produce HSV-1 proteins. Our goal was to define more precisely which class of viral gene products are associated with apoptosis prevention. The apoptotic viruses *d27-1*, *d1-5*, *d1-2*, *n263R*, and *n59R* had reduced levels of almost all of the viral proteins examined. In contrast, the apoptotic or partially apoptotic viruses M11, M15, M16, *n504R*, and *n406R* produced high levels of ICP4 and ICP22, reduced amounts of TK, VP16, and gD, but very little if any gC. It is noteworthy that these findings indicate that the protein reductions observed with apoptotic viruses are not simply due to loss of material as a result of cell death since wild-type levels of some viral proteins can be detected. Overall, there was a very good correlation between apoptosis prevention and the accumulation of early/leaky-late gene products TK, VP16, and gD. However, this conclusion remains a correlation and it must be emphasized that it is still possible that ICP27 is acting directly as well. These results suggest that in order for HSV-1 to prevent apoptosis, it must efficiently transit from the IE to E phase of replication.

(iv) ICP27 contains regions which are not required for prevention of apoptosis. The series of ICP27 mutants helps us to define the regions of ICP27 needed for apoptosis prevention as well as those regions which play minor or no roles. Our results indicate that a large region in ICP27 corresponding to amino acids 64 to 200 does not play a significant role in ICP27's ability to block apoptosis. This region is defined by recombinant viruses *d2-3*, *d3-4*, *d4-5*, *d5-6*, and *d6-7*, which were all found to be nonapoptotic. Of this group, only *d4-5* has a significant growth defect in Vero cells. The mutation in *d3-4* affects the ICP27 NLS (Fig. 1) and, consequently, increased amounts of ICP27 can be detected in the cytoplasm (36). However, significant ICP27 enters the nucleus in *d3-4*-infected cells due to nuclear localization signals present in the carboxy-terminal half of the protein (36), and the virus replicates in Vero cells (Table 2). It is noteworthy that the sequences deleted in *d3-4* and *d4-5* make up ICP27's NuLS (Fig. 1). We can thus conclude that nucleolar localization is not required for apoptosis prevention. The functions of the regions mutated in *d2-3*, *d5-6*, and *d6-7* remain unknown. Interestingly, while *d2-3* and *d3-4* produced wild-type levels of gC, ICP22 accumulations were reduced with these viruses. This supports our previous observation that while ICP22 may be involved in apoptosis prevention, it does not play a dominant role (2).

(v) The ICP27 RGG box is required for gC production but not for apoptosis prevention. It is interesting that the nonapoptotic virus *d4-5* has a deletion of the sequences encoding the RGG box region, which was shown to be (i) involved in RNA binding in vitro (38) and in vivo (56) and (ii) required for efficient viral growth in Vero cells (Table 2 [36]). Therefore, these results suggest that ICP27's direct interaction with RNA is not necessary for apoptosis prevention. However, we cannot exclude the possibility that additional potential RNA binding sites in ICP27 such as K homology-like domains (61, 62) might compensate for the loss of the RNA binding function of the RGG box. We also found that the RGG box region is not required for the efficient synthesis of ICP4, ICP22, TK, VP16, or gD. However, it is required for the efficient production of the true late gC protein, suggesting that ICP27's RNA binding activity is required for the induction of true late genes (48, 53). Since *d4-5* prevents apoptosis but cannot synthesize gC, the

results obtained using this virus functionally separate these two activities of ICP27.

(vi) ICP27's ability to prevent apoptosis requires functional regions in both the amino- and carboxy-terminal halves of the protein. Vero cells have the distinction of being unable to undergo apoptosis following ICP27-null virus infection (1). Thus, virus growth in Vero cells is an ideal assay to assess the consequences of ICP27 mutations on viral replication since infection occurs in a nonapoptotic cellular environment. For example, previous studies by one of us using Vero cells demonstrated that the M11, M15, M16, and *n504R* viruses replicate viral DNA (Table 1) but do not exhibit gC gene expression (48, 49). We have now compared the growth of various ICP27 mutants in Vero cells with their apoptotic potential in HEp-2 cells. With one exception, ICP27 mutants which are defective for plaque formation in Vero cells are also unable to mediate the activity which prevents apoptosis. The exception is *d4-5*, discussed above (sections iv and v). The apoptotic mutants included those with alterations in both the amino-terminal (e.g., *d1-2* and *d1-5*) and carboxy-terminal (e.g., M15 and *n504R*) parts of the protein. The mutations in *d1-5* and *d1-2* affect the ICP27 NES, leading to defects in shuttling, and the acidic regulation domain (50). Recent evidence indicates that this region also contains an export control sequence which appears to regulate the function of the NES (62). It is noteworthy that *d1-5* has a more pronounced apoptotic phenotype than *d1-2*, suggesting that residues 63 to 152 (Table 1) play a role in apoptosis prevention under some circumstances. All of the mutations which affect the carboxy-terminal portion of ICP27 resulted in a loss of the ability to prevent apoptosis. This is perhaps not surprising, as many previous data suggest that important functional regions lie in this domain. Interestingly, M11, M15, and M16 are deficient for ICP27 shuttling between the nucleus and cytoplasm of infected cells (37). ICP27 shuttling seems to be an event which occurs late in infection and plays a role in regulating late genes by facilitating export of mRNAs (43, 56, 60). However, since *n504R* still allows ICP27 to shuttle (37) and does not block apoptosis, the role of ICP27 shuttling in apoptosis prevention remains unclear.

Recently, another study (10) examined the ability of ICP27 mutants to promote the accumulation of unspliced cellular alpha-globin transcripts in infected HeLa cells, an activity which is dependent on ICP27 (14a). In this experimental system, all mutants which were defective for growth in Vero cells, including *d4-5*, were unable to promote accumulation of unspliced alpha-globin transcripts. These differing results underscore the fact that ICP27 is a complex protein comprised of multiple functional regions. In summary, our current data imply that the amino-terminal half of ICP27, like its carboxy-terminal half, possesses multiple regulatory regions which contribute to ICP27's role in apoptosis prevention.

(vii) Definition of apoptosis during HSV-1 infection and proposal of a model for apoptosis prevention by HSV-1. We found that all HEp-2 monolayers, including mock-infected ones, display some cells with distinguishing cell morphologies indicative of apoptosis. To differentiate between the phenotypes of apoptotic, partially apoptotic, and nonapoptotic mutants, it was therefore important to quantitatively determine the proportion of cells with apoptotic features. It should be noted that we use MOIs of at least 5 PFU/cell, and therefore

all cells in a given monolayer are infected. Viruses which are not able to prevent apoptosis (apoptotic or partially apoptotic) trigger greater than 30% of the cell population to have condensed chromatin. Extracts made from cells infected by these viruses display a significant level of processing of cellular death factors. In contrast, nonapoptotic viruses generate less than 20% apoptotic cells. For comparison, wild-type KOS1.1 infection produces 8% apoptotic cells in this system. Viral features which do not seem to be associated with apoptosis prevention include accumulations of ICP4 and ICP22, the act of viral DNA synthesis, and the production of true late proteins.

The prevention of apoptosis during HSV-1 infection is dependent upon the accumulation of early and leaky-late genes products. We propose (Fig. 9) that ICP27 stimulates the expression of these factors. This model is in agreement with the finding that the "preventer" of apoptosis is a protein synthesized between 3 and 6 h p.i. (2) and does not exclude a direct role for ICP27 or cellular factors in the prevention process. It is conceivable that ICP27 orchestrates the synthesis of multiple viral factors which block apoptosis in HSV-1-infected cells, making it the central regulatory player in the prevention process. In comparison, viruses producing nonfunctional forms of ICP4 accumulate large amounts of IE proteins, including ICP27, but are strictly blocked from synthesizing gene products of the later kinetic classes (12–14). Interestingly, HEp-2 cells infected with an ICP4-null virus were recently shown by us (M. Aubert et al., unpublished results) and others (16) to also undergo apoptosis. That ICP4-defective viruses make ICP27 yet fail to block apoptosis supports our model in which ICP27 prevents apoptosis indirectly by inducing the production early and leaky-late proteins.

Consistent with the hypothesis that ICP27 may activate multiple viral preventers is the fact that single genes (e.g., ICP22 or U_S3) have only minor roles in the prevention of apoptosis compared to that of ICP27 (2). Accordingly, these accessory genes may be deleted from the HSV-1 genome without having detrimental effects on viral replication in cultured cells (26, 27, 45, 46). It has also recently been suggested that the LAT RNAs may have an antiapoptotic function as this RNA can inhibit ceramide-, fumonisin-, and etoposide-induced apoptosis in transient expression assays (40). We have observed that at late infection times (9 h p.i.) in Vero cells, KOS1.1 produces high levels of the 2.0-kb LAT transcript, while this RNA is essentially absent with *d27-1*, *n504R*, *n406R*, *n263R*, and *n59R* (S. A. Rice, and D. M. Knipe, unpublished results). In addition, no LAT is detected during KOS1.1 infection in the presence of PAA, indicating that LAT is expressed with true late kinetics in Vero cells (Rice and Knipe, unpublished). We observed that HEp-2 cells infected by KOS1.1 in the presence of PAA acid do not undergo apoptosis (Fig. 8). Thus, if LAT has the same regulation in HEp-2 cells as in Vero cells, it is probably not the preventer since it would not be made in the presence of PAA.

While significant caspase-3 processing is detected by 11 h p.i. during wild-type KOS1.1 infection, few or no morphological signs of apoptosis are observed, even at 24 h (2). Based on this observation, we concluded (2) that infection by HSV-1 triggers the conversion of pro-caspase-3 to caspase-3 (Fig. 9). It is intriguing that *d4-5*-infected HEp-2 cells have less processing of caspase-3 than those infected with KOS1.1. We observed a

Apoptosis During Productive Herpes Simplex Virus Infection

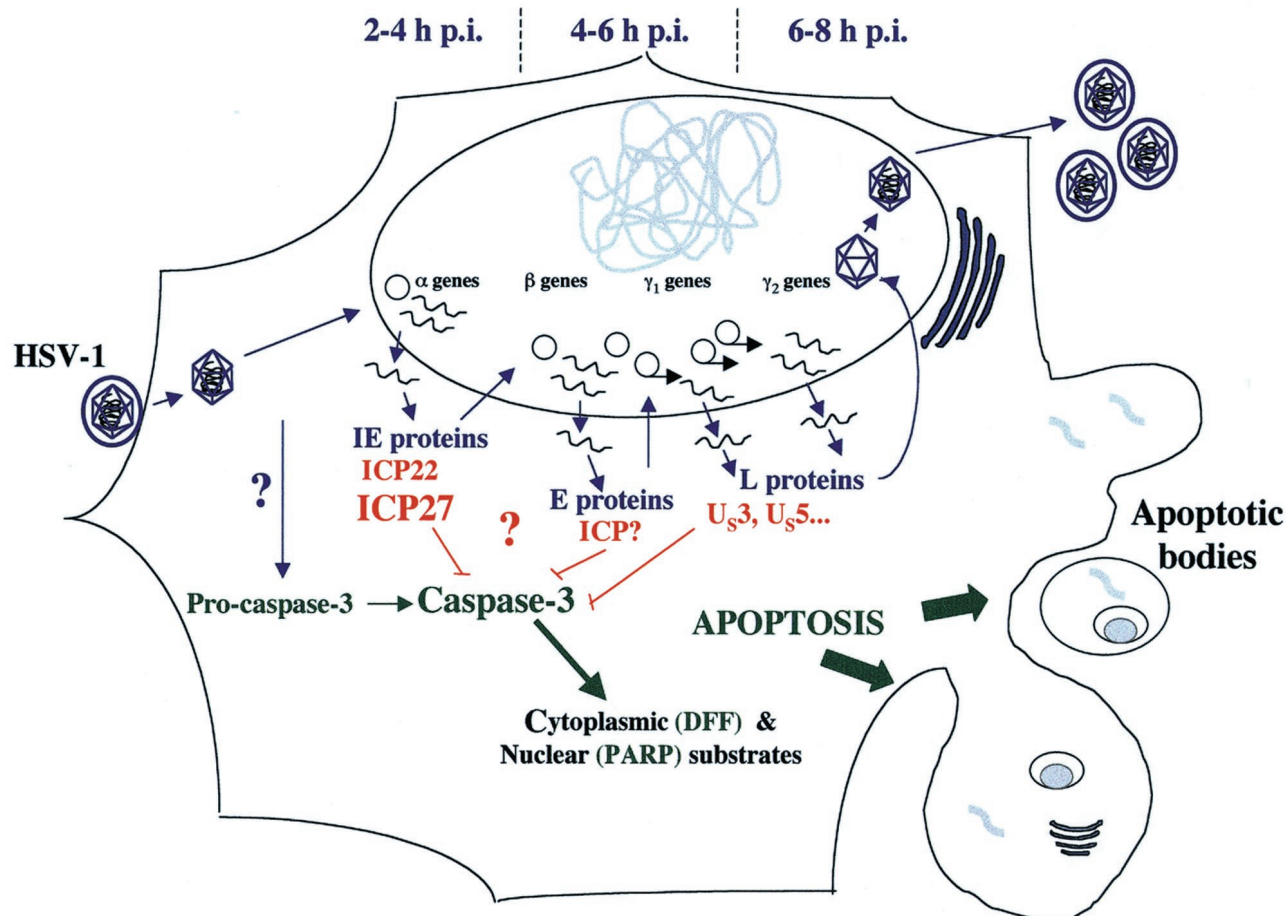


FIG. 9. Schematic representation of apoptosis during productive HSV-1 infection. HSV-1 replication occurs in a sequentially ordered cascade (23, 52). Following virion binding and fusion at the cell surface, tegument dissociation, capsid translocation to the nuclear pore, viral DNA release, and circularization in the nucleus, α gene expression occurs. Viral DNA synthesis begins after β gene expression. Expression of γ_2 genes is distinguished from that of γ_1 genes by its absolute dependence on viral DNA synthesis. Infection of HEP-2 cells with HSV-1 leads to the activation of caspase-3. Under conditions in which de novo viral protein synthesis is blocked (e.g., by addition of cycloheximide) or ICP27 is absent, activated caspase-3 cleaves cytoplasmic and nuclear substrates leading to the classic structural features of apoptosis, including chromatin condensation, nuclear fragmentation, nucleosomal DNA laddering, membrane blebbing, and the formation of apoptotic bodies (1). During infection with wild-type HSV-1, infected cell proteins synthesized between 3 and 6 h p.i. are capable of preventing the process from killing the cells (2). The data in this study indicate that the accumulation of viral early (β) and leaky-late (γ_1) proteins correlates with the prevention activity.

similar pattern using a *vhs*-deletion virus (2). As *vhs* enters the cell at the initial stage of infection, we suspected that *vhs* might have a role in the induction of apoptosis. However, since we have now obtained very similar results with a different mutant virus, we suggest the following to explain our findings. Since ICP27-null viruses stimulate apoptosis, the decreased level of apoptosis with *d4-5* is probably not due to reduced induction of the process. Because ICP27-dependent gene regulation is required for apoptosis prevention, we suggest that in *d4-5*-infected HEP-2 cells the preventer may accumulate to levels greater than in wild-type-virus-infected cells. Thus, the ICP27 region mutated in *d4-5* may function in regulating the balance between pro- and antiapoptotic factors during infection. According to this model, the *vhs*-deletion virus exhibits less apoptosis than the wild type because it induces a transition from E to L that is not sharp, consequently resulting in the accumu-

lation of the preventer. While our data favor such a scenario, we cannot exclude the possibility that infections with the *vhs*-deletion and *d4-5* mutant viruses lead to a decrease of an apoptotic activator. Alternatively, the induction process might involve the shutoff of a short-lived host protein that is protective.

In summary, experiments using a series of viral ICP27 mutants have identified regions in ICP27 which are both essential and nonessential for apoptosis prevention in infected human epithelial cells. Interestingly, a large portion of the amino-terminal half of the protein, including its known RNA binding domain, is not required for the prevention of apoptosis. In addition, prevention of apoptosis does not require the process of viral DNA synthesis itself nor the ability to synthesize gC and similar true late gene products. Our analyses show that a strong correlation exists between the ability of ICP27 mutants to stimulate the production of viral early/leaky-late proteins

and their ability to block apoptosis. Thus, we propose that ICP27 functions indirectly to prevent apoptosis by stimulating the synthesis of one or more viral inhibitors of apoptosis. Additional studies will be required to confirm our model and identify the putative inhibitory molecule(s).

ACKNOWLEDGMENTS

We thank Jennifer O'Toole for expert technical assistance and Scott Henderson for help in creating the Quicktime movie.

These studies were supported by grants AI38873 (to J.A.B.) and AI42737 (to S.A.R.) from the NIH. J.A.B. thanks the American Cancer Society (JFRA634), the National Foundation for Infectious Diseases, and the Lucille P. Markey Charitable Trusts for their support.

REFERENCES

- Aubert, M., and J. A. Blaho. 1999. The herpes simplex virus type 1 regulatory protein ICP27 is required for the prevention of apoptosis in infected human cells. *J. Virol.* **73**:2803–2813.
- Aubert, M., J. O'Toole, and J. A. Blaho. 1999. Induction and prevention of apoptosis in human HEP-2 cells by herpes simplex virus type 1. *J. Virol.* **73**:10359–10370.
- Avitabile, E., S. Di Gaeta, M. R. Torrisi, P. L. Ward, B. Roizman, and G. Campadelli-Fiume. 1995. Redistribution of microtubules and Golgi apparatus in herpes simplex virus-infected cells and their role in viral exocytosis. *J. Virol.* **69**:7472–7482.
- Batterson, W., and B. Roizman. 1983. Characterization of the herpes simplex virion-associated factor responsible for the induction of alpha genes. *J. Virol.* **46**:371–377.
- Blaho, J. A., C. Mitchell, and B. Roizman. 1993. Guanylation and adenylation of the alpha regulatory proteins of herpes simplex virus require a viral beta or gamma function. *J. Virol.* **67**:3891–3900.
- Blaho, J. A., C. S. Zong, and K. A. Mortimer. 1997. Tyrosine phosphorylation of the herpes simplex virus type 1 regulatory protein ICP22 and a cellular protein which shares antigenic determinants with ICP22. *J. Virol.* **71**:9828–9832.
- Boehmer, P. E., and I. R. Lehman. 1997. Herpes simplex virus DNA replication. *Annu. Rev. Biochem.* **66**:347–384.
- Brown, C. R., M. S. Nakamura, J. D. Mosca, G. S. Hayward, S. E. Straus, and L. P. Perera. 1995. Herpes simplex virus trans-regulatory protein ICP27 stabilizes and binds to 3' ends of labile mRNA. *J. Virol.* **69**:7187–7195.
- Chapman, C. J., J. D. Harris, M. A. Hardwicke, R. M. Sandri-Goldin, M. K. Collins, and D. S. Latchman. 1992. Promoter-independent activation of heterologous virus gene expression by the herpes simplex virus immediate-early protein ICP27. *Virology* **186**:573–578.
- Cheung, P., K. S. Ellison, R. Verity, and J. R. Smiley. 2000. Herpes simplex virus ICP27 induces cytoplasmic accumulation of unspliced polyadenylated α -globin pre-mRNA in infected HeLa cells. *J. Virol.* **74**:2913–2919.
- Cryns, V., and J. Yuan. 1998. Proteases to die for. *Genes Dev.* **12**:1551–1570.
- DeLuca, N. A., M. A. Courtney, and P. A. Schaffer. 1984. Temperature-sensitive mutants in herpes simplex virus type 1 ICP4 permissive for early gene expression. *J. Virol.* **52**:767–776.
- DeLuca, N. A., A. M. McCarthy, and P. A. Schaffer. 1985. Isolation and characterization of deletion mutants of herpes simplex virus type 1 in the gene encoding immediate-early regulatory protein ICP4. *J. Virol.* **56**:558–570.
- DeLuca, N. A., and P. A. Schaffer. 1985. Activation of immediate-early, early, and late promoters by temperature-sensitive and wild-type forms of herpes simplex virus type 1 protein ICP4. *Mol. Cell. Biol.* **5**:1997–2008.
- Ellison, K. S., S. A. Rice, and J. R. Smiley. 2000. Processing of α -globin and ICP0 mRNA in cells infected with herpes simplex virus type 1 ICP27 mutants. *J. Virol.* **74**:7307–7319.
- Fenwick, L. M., and M. J. Walker. 1978. Suppression of the synthesis of cellular macromolecules by herpes simplex virus. *J. Gen. Virol.* **41**:37–51.
- Galvan, V., R. Brandimarti, J. Munger, and B. Roizman. 2000. Bcl-2 blocks a caspase-dependent pathway of apoptosis activated by herpes simplex virus 1 infection in HEP-2 cells. *J. Virol.* **74**:1931–1938.
- Green, D. R. 1998. Apoptotic pathways: the roads to ruin. *Cell* **94**:695–698.
- Hampar, B., and S. A. Elison. 1961. Chromosomal aberrations induced by an animal virus. *Nature* **192**:145–147.
- Hardwicke, A. M., P. J. Vaughan, R. E. Sekulovich, R. O'Conner, and R. M. Sandri-Goldin. 1989. The regions important for the activator and repressor functions of herpes simplex virus type 1 alpha protein ICP27 map to the C-terminal half of the molecule. *J. Virol.* **63**:4590–4602.
- Hardy, W. R., and R. M. Sandri-Goldin. 1994. Herpes simplex virus inhibits host cell splicing, and regulatory protein ICP27 is required for this effect. *J. Virol.* **68**:7790–7799.
- Heeg, U., H. P. Dienes, S. Muller, and D. Falke. 1986. Involvement of actin-containing microfilaments in HSV-induced cytopathology and the influence of inhibitors of glycosylation. *Arch. Virol.* **91**:257–270.
- Hibbard, K. M., and R. M. Sandri-Goldin. 1995. Arginine-rich regions succeeding the nuclear localization region of the herpes simplex virus type 1 regulatory protein ICP27 are required for efficient nuclear localization and late gene expression. *J. Virol.* **69**:4656–4667.
- Honess, R. W., and B. Roizman. 1974. Regulation of herpesvirus macromolecular synthesis. I. Cascade regulation of the synthesis of three groups of viral proteins. *J. Virol.* **14**:8–19.
- Hughes, R. G., Jr., and W. H. Munyon. 1975. Temperature-sensitive mutants of herpes simplex virus type 1 defective in lysis but not in transformation. *J. Virol.* **16**:275–283.
- Ingram, A., A. Phelan, J. Dunlop, and J. B. Clements. 1996. Immediate early protein IE63 of herpes simplex virus type 1 binds RNA directly. *J. Gen. Virol.* **77**:1847–1851.
- Javier, R. T., J. G. Stevens, V. B. Dissette, and E. K. Wagner. 1988. A herpes simplex virus transcript abundant in latently infected neurons is dispensable for establishment of the latent state. *Virology* **166**:254–257.
- Jerome, K. R., R. Fox, Z. Chen, A. E. Sears, H. Lee, and L. Corey. 1999. Herpes simplex virus inhibits apoptosis through the action of two genes, Us5 and Us3. *J. Virol.* **73**:8950–8957.
- Kerr, J. F., and B. V. Harmon. 1991. Definition and incidence of apoptosis: an historical perspective, p. 5–29. *In* L. D. Tomei and F. O. Cope (ed.), *Apoptosis: the molecular basis of cell death*. Cold Spring Harbor Laboratory, Cold Spring Harbor, N.Y.
- Kerr, J. F., A. H. Wyllie, and A. R. Currie. 1972. Apoptosis: a basic biological phenomenon with wide-ranging implications in tissue kinetics. *Br. J. Cancer* **26**:239–257.
- Koyama, A. H., and A. Adachi. 1997. Induction of apoptosis by herpes simplex virus type 1. *J. Gen. Virol.* **78**:2909–2912.
- Liu, X., H. Zou, C. Slaughter, and X. Wang. 1997. DFF, a heterodimeric protein that functions downstream of caspase-3 to trigger DNA fragmentation during apoptosis. *Cell* **89**:175–184.
- McCarthy, A. M., L. McMahan, and P. A. Schaffer. 1989. Herpes simplex virus type 1 ICP27 deletion mutants exhibit altered patterns of transcription and are DNA deficient. *J. Virol.* **63**:18–27.
- McGregor, F., A. Phelan, J. Dunlop, and J. B. Clements. 1996. Regulation of herpes simplex virus poly(A) site usage and the action of immediate-early protein IE63 in the early-late switch. *J. Virol.* **70**:1931–1940.
- McLaughlan, J., A. Phelan, C. Loney, R. M. Sandri-Goldin, and J. B. Clements. 1992. Herpes simplex virus IE63 acts at the posttranscriptional level to stimulate viral mRNA 3' processing. *J. Virol.* **66**:6939–6945.
- McMahan, L., and P. A. Schaffer. 1990. The repressing and enhancing functions of the herpes simplex virus regulatory protein ICP27 map to C-terminal regions and are required to modulate viral gene expression very early in infection. *J. Virol.* **64**:3471–3485.
- Mears, W. E., V. Lam, and S. A. Rice. 1995. Identification of nuclear and nucleolar localization signals in the herpes simplex virus regulatory protein ICP27. *J. Virol.* **69**:935–947.
- Mears, W. E., and S. A. Rice. 1998. The herpes simplex virus immediate-early protein ICP27 shuttles between nucleus and cytoplasm. *Virology* **242**:128–137.
- Mears, W. E., and S. A. Rice. 1996. The RGG box motif of the herpes simplex virus ICP27 protein mediates an RNA-binding activity and determines in vivo methylation. *J. Virol.* **70**:7445–7453.
- Nicholson, D. W., and N. A. Thornberry. 1997. Caspases: killer proteases. *Trends Biochem. Sci.* **22**:299–306.
- Perng, G. C., C. Jones, J. Ciacci-Zanella, M. Stone, G. Henderson, A. Yukht, S. M. Stanina, F. M. Hofman, H. Ghiasi, A. B. Nesburn, and S. L. Wechsler. 2000. Virus-induced neuronal apoptosis blocked by the herpes simplex virus latency-associated transcript. *Science* **287**:1500–1503.
- Phelan, A., M. Carmo-Fonseca, J. McLaughlan, A. I. Lamond, and J. B. Clements. 1993. A herpes simplex virus type 1 immediate-early gene product, IE63, regulates small nuclear ribonucleoprotein distribution. *Proc. Natl. Acad. Sci. USA* **90**:9056–9060.
- Phelan, A., and J. B. Clements. 1997. Herpes simplex virus type 1 immediate early protein IE63 shuttles between nuclear compartments and the cytoplasm. *J. Gen. Virol.* **78**:3327–3331.
- Phelan, A., J. Dunlop, and J. B. Clements. 1996. Herpes simplex virus type 1 protein IE63 affects the nuclear export of virus intron-containing transcripts. *J. Virol.* **70**:5255–5265.
- Pomeranz, L. E., and J. A. Blaho. 1999. Modified VP22 localizes to the cell nucleus during synchronized herpes simplex virus type 1 infection. *J. Virol.* **73**:6769–6781.
- Post, L. E., and B. Roizman. 1981. A generalized technique for deletion of specific genes in large genomes: alpha gene 22 of herpes simplex virus 1 is not essential for growth. *Cell* **25**:227–232.
- Purves, F. C., R. M. Longnecker, D. P. Leader, and B. Roizman. 1987. Herpes simplex virus 1 protein kinase is encoded by open reading frame US3 which is not essential for virus growth in cell culture. *J. Virol.* **61**:2896–2901.
- Read, G. S., B. M. Karr, and K. Knight. 1993. Isolation of a herpes simplex virus type 1 mutant with a deletion in the virion host shutoff gene and

- identification of multiple forms of the *vhs* (UL41) polypeptide. *J. Virol.* **67**:7149–7160.
48. **Rice, S. A., and D. M. Knipe.** 1990. Genetic evidence for two distinct trans-activation functions of the herpes simplex virus alpha protein ICP27. *J. Virol.* **64**:1704–1715.
 49. **Rice, S. A., and V. Lam.** 1994. Amino acid substitution mutations in the herpes simplex virus ICP27 protein define an essential gene regulation function. *J. Virol.* **68**:823–833.
 50. **Rice, S. A., V. Lam, and D. M. Knipe.** 1993. The acidic amino-terminal region of herpes simplex virus type 1 alpha protein ICP27 is required for an essential lytic function. *J. Virol.* **67**:1778–1787.
 51. **Rice, S. A., L. S. Su, and D. M. Knipe.** 1989. Herpes simplex virus alpha protein ICP27 possesses separable positive and negative regulatory activities. *J. Virol.* **63**:3399–3407.
 52. **Roizman, B., and A. Sears.** 1996. Herpes simplex viruses and their replication, p. 2231–2295. *In* B. N. Fields and D. M. Knipe (ed.), *Virology*, 3rd ed. Lippincott-Raven, Philadelphia, Pa.
 53. **Sacks, W. R., C. C. Greene, D. P. Aschman, and P. A. Schaffer.** 1985. Herpes simplex virus type 1 ICP27 is an essential regulatory protein. *J. Virol.* **55**:796–805.
 54. **Salvesen, G. S., and V. M. Dixit.** 1997. Caspases: intracellular signaling by proteolysis. *Cell* **91**:443–446.
 55. **Samaniego, L. A., A. L. Webb, and N. A. DeLuca.** 1995. Functional interactions between herpes simplex virus immediate-early proteins during infection: gene expression as a consequence of ICP27 and different domains of ICP4. *J. Virol.* **69**:5705–5715.
 56. **Sandri-Goldin, R. M.** 1998. ICP27 mediates HSV RNA export by shuttling through a leucine-rich nuclear export signal and binding viral intronless RNAs through an RGG motif. *Genes Dev.* **12**:868–879.
 57. **Sandri-Goldin, R. M., M. K. Hibbard, and M. A. Hardwicke.** 1995. The C-terminal repressor region of herpes simplex virus type 1 ICP27 is required for the redistribution of small nuclear ribonucleoprotein particles and splicing factor SC35; however, these alterations are not sufficient to inhibit host cell splicing. *J. Virol.* **69**:6063–6076.
 58. **Sandri-Goldin, R. M., and G. E. Mendoza.** 1992. A herpesvirus regulatory protein appears to act post-transcriptionally by affecting mRNA processing. *Genes Dev.* **6**:848–863.
 59. **Sekulovich, R. E., K. Leary, and R. M. Sandri-Goldin.** 1988. The herpes simplex virus type 1 alpha protein ICP27 can act as a trans-repressor or a trans-activator in combination with ICP4 and ICP0. *J. Virol.* **62**:4510–4522.
 60. **Soliman, T. M., R. M. Sandri-Goldin, and S. J. Silverstein.** 1997. Shuttling of the herpes simplex virus type 1 regulatory protein ICP27 between the nucleus and cytoplasm mediates the expression of late proteins. *J. Virol.* **71**:9188–9197.
 61. **Soliman, T. M., and S. J. Silverstein.** 2000. Herpesvirus mRNAs are sorted for export via Crm1-dependent and -independent pathways. *J. Virol.* **74**:2814–2825.
 62. **Soliman, T. M., and S. J. Silverstein.** 2000. Identification of an export control sequence and a requirement for the KH domains in ICP27 from herpes simplex virus type 1. *J. Virol.* **74**:7600–7609.
 63. **Tewari, M., D. R. Beidler, and V. M. Dixit.** 1995. CrmA-inhibitable cleavage of the 70-kDa protein component of the U1 small nuclear ribonucleoprotein during Fas- and tumor necrosis factor-induced apoptosis. *J. Biol. Chem.* **270**:18738–18741.
 64. **Tewari, M., W. G. Telford, R. A. Miller, and V. M. Dixit.** 1995. CrmA, a poxvirus-encoded serpin, inhibits cytotoxic T-lymphocyte-mediated apoptosis. *J. Biol. Chem.* **270**:22705–22708.
 65. **Uprichard, S. L., and D. M. Knipe.** 1996. Herpes simplex ICP27 mutant viruses exhibit reduced expression of specific DNA replication genes. *J. Virol.* **70**:1969–1980.
 66. **Vaughan, P. J., K. J. Thibault, M. A. Hardwicke, and R. M. Sandri-Goldin.** 1992. The herpes simplex virus immediate early protein ICP27 encodes a potential metal binding domain and binds zinc in vitro. *Virology* **189**:377–384.
 67. **Wilcox, K. W., A. Kohn, E. Sklyanskaya, and B. Roizman.** 1980. Herpes simplex virus phosphoproteins. I. Phosphate cycles on and off some viral polypeptides and can alter their affinity for DNA. *J. Virol.* **33**:167–182.
 68. **Wyllie, A. H., J. F. Kerr, and A. R. Currie.** 1980. Cell death: the significance of apoptosis. *Int. Rev. Cytol.* **68**:251–306.
 69. **Zhi, Y., and R. M. Sandri-Goldin.** 1999. Analysis of the phosphorylation sites of herpes simplex virus type 1 regulatory protein ICP27. *J. Virol.* **73**:3246–3257.